PREPARATION AND CHARACTERIZATION OF CERAMIC MICRO/ULTRA/NANOFILTRATION MEMBRANES FOR SEPARATION PROCESSES AND WASTEWATER TREATMENT

A Thesis Submitted to
The Graduate School of Engineering and Sciences of
İzmir Institute of Technology
in Partial Fulfillment of the Requirements for the Degree of

MASTER OF SCIENCE

in Materials Science and Engineering

By
Öncel KIRKBAŞ

April 2016
İZMİR

We approve the thesis of **Öncel KIRKBAŞ**

Examining Committee Members:

_____

Prof. Dr. Muhsin ÇİFTÇİOĞLU
Department of Chemical Engineering, İzmir Institute of Technology

_____

Assist. Prof.Dr. Umut ADEM
Department of Materials Science and Engineering, İzmir Institute of Technology

_____

Assist.Prof.Dr.Mücahit SÜTÇÜ
Department of Materials Science and Engineering, İzmir Katip Çelebi University

12 April 2016

_____

Prof. Dr. Muhsin ÇİFTÇİOĞLU
Supervisor, Department of Chemical Engineering, İzmir Institute of Technology

_____

Prof. Dr. Mustafa Muammer DEMİR
Head of the Department of Materials Science and Engineering

_____

Prof. Dr. Bilge KARAÇALI
Dean of the Graduate School of Engineering and Sciences

ACKNOWLEDGEMENTS

I would like to express my deepest gratitude to my advisor, Prof. Dr. Muhsin ÇİFTÇİOĞLU for his guidance, support, motivation and encouragement during my thesis.

I would also like to thank Kenan YILMAZ, Kaan YALTRIK, Safiye YALDIZ, Iklima ODABAŞI, Ali Emrah ÇETİN, Rukiye ÇİFTÇİOĞLU and Burcu ALP for their assistance during this study.

I would like to thank İzmir Institute of Technology Environmental Development Application and Research Center for providing technical support and help.

Lastly, I offer sincere thanks to my family; Nihal KIRKBAŞ, Mehmet KIRKBAŞ, Necmiye OFOĞLU and Sami OFOĞLU for their love, continuous support and unlimited patience throughout my education.

This study was supported by The Scientific and Technological Research Council of Turkey (TUBITAK) within the context of ÇAYDAG 113Y344 project.

ABSTRACT

PREPARATION AND CHARACTERIZATION
OF CERAMIC
MICRO/ULTRA/NANOFILTRATION
MEMBRANES FOR SEPARATION PROCESSES AND
WASTEWATER TREATMENT

The availability of fresh water is vital for life, sustainable growth and healthy ecosystems on earth. Increasing world population, a changing climate, intensive agricultural practices, economic growth and urbanization will undoubtedly continue to make the issue of water scarcity a global priority for years to come. The gap between the need and the supply of water globally is increasing steadily which necessitates significant measures to be taken towards conservation, and reuse of industrially, domestically and agriculturally used water. Textile industry is one of the leading industries in the use of fresh water and the generation of wastewaters. Technologies currently in use towards industrial and domestic water treatment like sedimentation, chemical coagulation, biological treatment etc. cannot produce reusable water but also generate significant amounts of solid waste. Membranes are now widely accepted to have the potential of supplying cost-effective solutions for water treatment and a growing range of purification and separation problems.

The number and the pore structure design of the multiple selective layers on the inner surfaces of tubular α-alumina supports vary with the nature of the intended separation application. Although the nature of MF membranes is relatively well developed, current research is concentrated on the design of nanoporous phase structure in NF and UF selective layers.

Selective micro/ultra/nanofiltration layers were formed on extruded tubular alumina supports by colloidal/sol-gel techniques. The performance of these selective layers were investigated by the experiments performed with textile wastewater. Permeates from ceramic tubular membranes were characterized by spectrophotometer. The suspended solids and color (Pt-Co) were reduced by 90% and 80%. respectively.

ÖZET

SERAMİK MİKRO/ULTRA/NANOFİLTRASYON MEMBRANLARININ HAZIRLANMASI, KARAKTERİZASYONU VE AYIRMA İŞLEMLERİ, ATIKSU ARITIMINDA KULLANILMASI

Temiz suyun erişilebilirliği dünyamızdaki yaşam, sürdürülebilir büyüme, ve sağlıklı ekosistemler için hayati bir öneme sahiptir. İvmelenerek artan dünya nüfusu, değişen bir iklimin varlığı, yoğun tarımsal faaliyetler, ve şehirleşme hiç şüphesiz olarak öngörebildiğimiz yıllar boyunca suyun azlığı olgusunun küresel bir öncelik olmasına neden olmaya devam edecektir. Küresel olarak temiz su gereksinimi ve varlığı arasındaki giderek büyüyen açık, suyun korunumu, ve endüstriyel, evsel ve tarımsal amaçla kullanılan suyun geri kazanılarak kullanımı konusunda çok ciddi önlemlerin alınmasını zorunlu hale getirmektedir. Günümüzde endüstriyel ve evsel atık suyun arındırılmasında kullanılan çöktürme, kimyasal koagülasyon, biyolojik arıtma v.b. teknolojiler geri kullanılabilir özelliklerde su sağlayamadıkları gibi önemli miktarlarda katı atık da üretmektedirler. Su arıtma ve büyüyen bir kapsamdaki arıtma ve ayırma problemlerine membranların ekonomik çözümler üretme potansiyaline sahip oldukları artık yaygın bir biçimde kabul edilmiş durumdadır.

Çoklu seçici katmanların sayısı ve gözenek yapısı tasarımı hedeflenen ayırım uygulamasının niteliğine göre değişir. MF membranların yapısı göreceli olarak daha iyi gelişmiş ise de güncel araştırmalar NF ve UF seçici katmanların nanogözenekli faz yapısının tasarımı konusunda yoğunlaşmış durumdadır.

Ekstrüzyon yöntemi ile şekillendirilmiş seramik tübüler alümina destekler üzerine kolloidal/sol-jel teknikleri ile seçici mikro/ultra/nanofiltrasyon katmanları oluşturulmuştur. Seçici katmanların performansları tekstil atık suları ile incelenmiştir. Seramik tübüler membrandan elde edilen süzüntüler spektrofotometre ile karakterize edilmiştir. Bunun sonucunda askıda katı ve renk (Pt-Co) değerleri sırasıyla 90% ve 80% ‘e düşürülmüştür.

TABLE OF CONTENTS

LIST OF FIGURES

Figure **Page**

LIST OF TABLES

Table **Page**

CHAPTER 1

INTRODUCTION

The availability of fresh water is vital for life, sustainable growth and healthy ecosystems on earth. Increasing world population, a changing climate, intensive agricultural practices, economic growth and urbanization will undoubtedly continue to make the issue of water scarcity a global priority for years to come. The gap between the need and the supply of water globally is increasing steadily which necessitates significant measures to be taken towards conservation, and reuse of industrially, domestically and agriculturally used water. Technologies currently in use towards industrial and domestic water treatment like sedimentation, chemical coagulation, biological treatment etc. cannot produce reusable water but also generate significant amounts of solid waste. Membranes are now widely accepted to have the potential of supplying cost-effective solutions for water treatment and a growing range of purification and separation problems.

The industrial use of polymeric and inorganic membranes towards desalination and nuclear fuel enrichment started in the 1950s and 1960s. Although polymeric membranes still dominate the market, the share of the ceramic membranes is steadily increasing with the reduction of especially their initial costs. This increasing trend in ceramic membrane based separation applications originate from their superior thermal, chemical, mechanical properties and significantly longer service lifetimes relative to their polymeric counterparts.

The utilization of ceramic membranes in separation processes started in the 1980s and currently they are widely used in water treatment, food and beverage, chemical, pharmaceutical etc. industries. Metal, food, textile, pulp and paper industries are using large amounts of water. In recent years wastewater treatment technologies are focused on wastewater treatment of textile industry. Reuse of water in textile industry is around 1% which is the main motivation behind increasing attention on textile industry wastewater treatment research. European Union declared that the best treatment technique (BAT) for textile wastewater treatment is the membrandc,2

4e separation process in 1999 (Capar et al. 2008).The dye components of textile wastewater is concentrated and separated effectively by membrane processes. Ceramic membranes are also resistant to chemical and microbial attacks and high temperature (Damas et al. 2012). Nanofiltration which is a pressure driven membrane process has a high textile wastewater purification ability. Nanofiltration can separate particles 1nm ($10A^{o}$) in size with molecular weights as low as 200-1000 Da. The formation of a film of concentrated waste particles causing a significant level of fouling on the membrane surface and high cost of operation are the major disadvantages of membrane processes. Treatment performance of textile wastewater with ceramic ultrafiltration, nanofiltration and polymeric reverse osmosis membrane processes were investigated by Damas et al. (2012). They reported that decreasing the level of concentrate waste particle accumulation on the surface, fouling and flux decline problems can be solved by pre-treatment process prior to membrane treatment.

A number of companies in Germany, France, USA, Japan, etc. produce and supply MF-UF-NF ceramic membrane modules and their housings. These modules come in various geometries mostly tubular in shape with multichannels and are formed from selective thin layers on extruded α-Al_2O_3 supports. The number and the pore structure design of these multiple selective layers vary with the nature of the intended separation application. Although the nature of MF membranes is relatively well developed, current research is concentrated on the design of nanoporous phase structure in NF and UF selective layers.

In this study, MF-UF-NF selective layers were prepared by sol-gel techniques and alumina tubular supports were coated by dip coating method. The selective layers were further heat treated for thermal and structural stability. The wastewater was treated in cross flow operation by a pilot scale setup. Concentration and recycle mode of filtration experiments were conducted and retentate/permeate properties (Chemical oxygen demand, color, conductivity, suspended solids content, metal ion contents) were determined. Permeates were observed to meet the discharge criteria. Analysis of the various resistances to flow and fouling were conducted.

CHAPTER 2

GLOBAL WATER RESOURCES AND TEXTILE INDUSTRY

Total water reserve is 1.4 billion km^3 in the world. 97% of this reserve is composed of ocean and sea which are salty water; only 2.5% is fresh water of total water reserve. The limited fresh water causes unbalanced share of fresh water by different countries in the world mainly due to population growth and climate change. It is estimated that 7 billion people will be in water scarcity by 2025 which would be the reason of war and immigration. The humanity should immediately find a solution to this problem.

Table 2.1. Annual available water quantity per person in selected countries. (Source:DSI,2012)

Country	Avaliable water quantity [m^3]
Syria	1.200
Turkey	1.430
Asia	3.000
West Europe	5.000
Africa	7.000
World average	7.600

Most countries in the Near East and Africa are in the water scarcity region. Annual available water quantity per person in selected countries is given in Table 2.1 showing that Turkey is the poorest country in the Europe but on the other hand Turkey is the water-richest country in the Middle East. A country is considered to be water-rich if water quantity per person is in between 8000-10000 m^3 (Table 2.2.). These water quantity values are based on water reserves and the population of the countries. Water quantity of per person in Turkey is around 1430 m^3 which is under the world average of 7.600 m^3. Turkey is not a water rich country and is prone to water scarcity in the near future.

Turkey Statistical Institute (TUIK) declared that water quantity of per person in Turkey will be reduced from 1.430 to 1.120 m^3 in 2030 and Turkey will be in the water-scarcity zone which is illustrated in Figure 2.1. The rate of population growth and unconscious water use have placed a significant stress on the water reserves. Turkey Statistical Institute also indicated the possibility of preserving available water reserves up to 2030 by raising the awareness of society on the scarcity of water.(DSI, 2012).

Table 2.2. Assesment of annual avaliable water quantity per person. (Source:DSI,2012)

8000 - 10.000 m^3	Water Rich
2000 m^3 <	Water Scarcity
1000 m^3 <	Water Poor

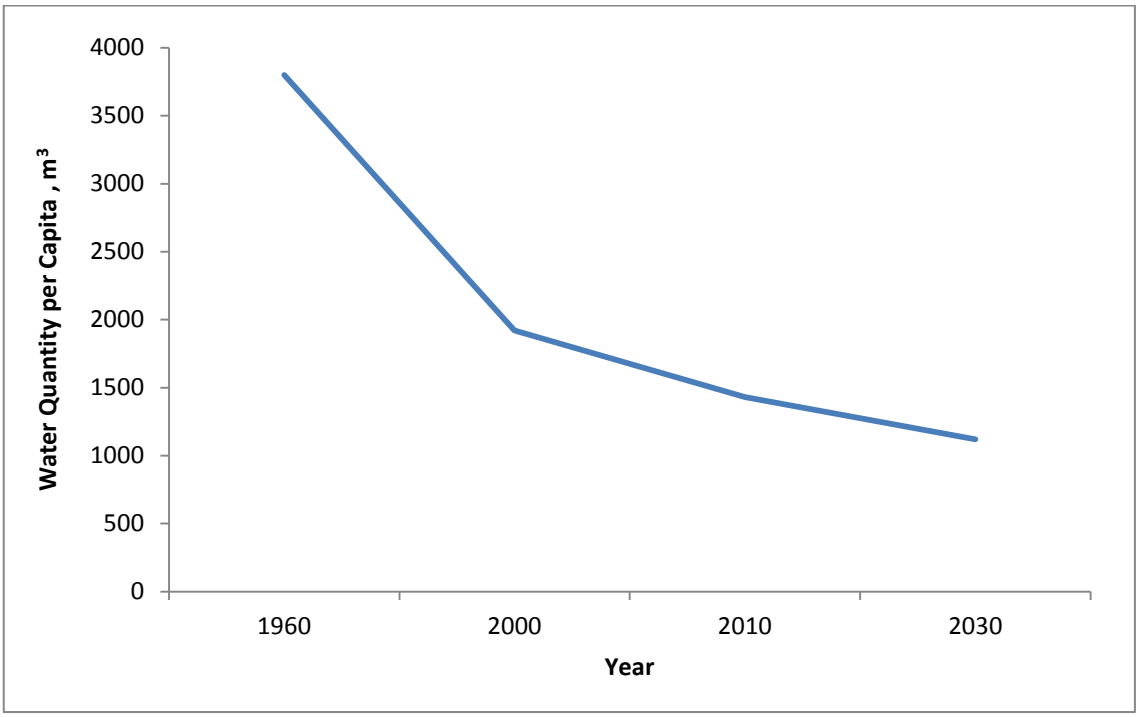

Figure 2.1. Changes and expectations of water quantity per person in Turkey. (Source:DSI,2012)

Communities on water around the world stated the importance of sustainable water technologies as a linkage between scarcity of water, public health, food and ecosystem. Water organizations heavily focused on sustainable water technologies in the last century with the emergence of new technologies and globalization. The global

and regional water organizations gathered in 7th World water forum for the first time towards formulating solutions to the global water issue in March 2015. These organizations was also involved in a prior meeting organized by UNESCO-world water assessment programme and Intergovernmental Panel on Climate Change (IPCC) in 2009. The 2015 forum was focused on increasing the limited water reserve awareness of society, water industries, wastewater treatment technologies and reuse strategies. The industry is putting an ever increasing pressure on the society. This leads to an increased level of sophisticated production towards satisfying the needs of the society which also increases water usage in industrial applications.

2.1 Textile Industry

Rapidly increasing population, intensified industrialization, and insufficient precipitation are restricting the availability of fresh water. The amount of industrial wastewater is increasing year by year and its discharge presents a very harmful effect on the limited fresh water reserves. Water pollutant control regulations define a series of 'colour parameters' as the major wastewater properties. Colour parameters for wastewater discharge in pulp and paper industry, textile industry, food industry are defined for the protection of clean water resources.

Table 2.3. Annual wastewater and treated wastewater amounts in selected industries. (Source:TUIK,2012)

Industry	**Total wastewater ($x10^4$ m^3)**	**Treated water ($x10^4$ m^3)**	**Percent of treated wastewater**
Metal industry	78300	36801	47%
Food industry	13484	260	2%
Pulp and paper industry	2100	546	26%
Textile industry	11324	113	1%

Metal, food, textile, pulp and paper industries are using large amounts of water. In recent years wastewater treatment technologies are heavily applied on wastewater generated in textile industry. This mainly is due to the very low treated water levels (about 1% of generated wastewater) in textile industry as given in Table 2.3 (TUIK,2012).

Degradation of textile dye effluents is very slow which causes toxic effects and poor water quality and apperance. Insufficient wastewater treatment is the major reason for the stable longterm presence of dye effluents in the environment for many years. Colour effluents even in less than 1ppm level can be easily recognizable in fresh water or nature (European commission, 2010). Direct discharge of dye wastewater decreases both the extent of photocatalytic organic waste decomposition activity and dissolved oxygen in nature along with negative health effects on population which may be mutagenic and carcinogenic. Chemical oxygen demand and suspended solid content are also valuable characterization parametres besides effluents colour parameters. Many countries prepared laws restricting the discharge of large amounts of colourful wastewater. Dye industries are forced to reuse water and reduce the amount of fresh water used in their processing (Schrank et al. 2007).

2.2 Properties and Sources of Textile Wastewater

The increase in the amout of textile wastewater is closely related with the increasing diversity and amount of textile products. The composition and quantity of textile wastewater show variability with the applied textile production technology. The nature and content of textile wastewater becomes more complex every year and vary with new production technologies and processes. Wastewaters mainly contain non-biodegradable organics, dye particles, inhibitor compounds and salts. The reference characterization values for water reuse in textile industry is given in Table 2.4.

Table 2.4. The reference wastewater reuse values for textile industry.
(Source: TUIK, 2012)

Parameter	Criteria
COD (mg/L)	250-400
pH	6-9
Turbidity (NTU)	1
Color (Pt-Co)	260-280
Suspended solids (mg/L)	140-400

The dyeing process involves encolouring of the fibre/fabric which is the fundamental process in textile industries. Dyes, tar and petrol based synthetic compounds are used in textile dyeing process. Dyes are resistant to ozone, peroxide, chlorine compounds and light. The amount of textile wastewater is related with dyeing bath and laundering or washing process (Schrank et al. 2007). Dyeing and laundering process wasewaters have low organic particle and high dye contents.

Compounds with many very different chemical groups are used in textile industry and they are present in wastewaters. Generally these chemical groups consist of functional and chromophore groups. The chromophore has more than one chemical bond and these chemical bonds are changeable. The chemical bonds of chromophore group which can absorb sun light providing brightness to the dye. The commonly used chromophore group is an azo-group. Other chemicals containing indigo and sulfur are also present in dye effluents and they assist in the absorbance of the dye by the fabric.

Global dye production is about one million tone in a year. Azo dyes constitute about 50%-60% of the total dye production which are mainly used in fabric or fibre dyeing. Chemical structure of indigo dye is shown in Figure 2.2.

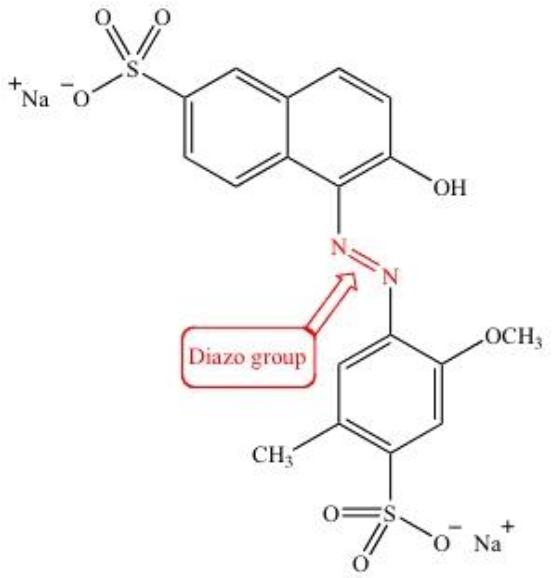

Figure 2.2. Chemical structure of indigo dye.

Generally indigo dyes are used in jean and other blue cotton clothes fabric. Indigo dye application procedure is complex since they do not easily dissolve in water. Indigo dye can be dissolved in water by a reduction reaction. The reduction reaction is realised by sodium dithionite ($Na_2S_2O_4$). These chemicals and reaction compounds also cause difficulties in the treatment of wastewater by using classical methods.

2.3 Wastewater Treatment Technologies in Textile Industry

The improvement of efficient and low cost water purification technologies are constrained by restricted regulations of water discharge and limited fresh water reserves. Another alternative approach is reuse of process water. Physico-chemical treatment, biological treatment and combination of both treatment technologies are used for reuse of process water. Textile wastewater treatment techniques can be classified in three groups as:

- Biological treatment
- Physico-chemical treatment
- Membrane technology

Biological treatment generates lower amounts of sludge compared to physicochemical treatment. Other advantages of biological treatment are its low operational cost, harmless waste product and eco-friendly nature. Biological treatment is commonly used in wastewater treatment applications. Textile wastewater contains molecular species with molecular weights in the 200-400 Da range. Biological treatment may be ineffective for complete removal of these species. Separation principle of biological treatment is based on microbial activities. The effluents in wastewater is consumed by bacteria, algae and fungi in biological treatment. Ahmad (2005) investigated reclamation of textile wastewater by biological treatment. The effluents of textile water were textile azo dyes which were CI reactive yellow 107,CI reactive black 5,CI reactive red 198 and CI direct blue 71 (Ahmad et al. 2005).

Physicochemical treatment is commonly used in dye industries. Processes of physico-chemical treatment include coagulant, decolorant or coagulation, electrocoagulation, flocculation or sedimentation which is conducted by the addition polymeric compounds. The character of textile wastewater is changed by physicochemical treatment. Phycsicochemical treatment is more efficient than biological treatment, on the other hand high cost and requirement of chemical additives are disadvantages of pycsico-chemical treatment (Uzal et al. 2009). Egerton investigated reclamation of textile wastewater by physicochemical treatment. The effluent of textile water was reactive orange 16 azo dyes (Egerton et al. 2014).

Europen Union declared that the best treatment technique (BAT) of textile wastewater was membrane separation process in 1999 (Capar et al. 2008). The dyes present in textile wastewaters can be separated and concentrated effectively by membrane processes. Ceramic membrane separation process is also resistant to chemical and microbial attacks and heat (Damas et al. 2012). Nanofiltration which is a pressure driven membrane process have a high separation ability in the treatment of textile wastewater. Nanofiltration can separate particles with sizes as low as 1nm and molecular species with molecular weights in the 200-400 nm range. The accumulation of effluent particles on the membrane surface causing fouling and the high initial cost of the operations are the major disadvantages of the membrane processes. Treatment of textile wastewater with ceramic ultrafiltration, nanofiltration and polymeric reverse osmosis was conducted and their performances were determined (Damas et al. 2012). The reduction of the accumulation of concentrate waste on membrane surface, fouling

and flux decline problems can be significantly reduced by using pre-treatment processes (Damas et al. 2012).

CHAPTER 3

MEMBRANE TECHNOLOGY

3.1 Membrane Working Principle

Membranes have a semi-permeable construction. Wastewater is separated to a retentate and a permeate stream. The driving forces for the separation process can be pressure, concentration, temperature and electrical potential. The majority of the membrane processes in wastewater treatment are pressure driven. The membrane allows passage of permeable components whereas impermeable components are held in the retentate. The waste retentate stream is rich in impermeable ingredients while the purified stream is quite poor in impermeable ingredients.

Microfiltration (MF), ultrafiltration (UF), nanofiltration (NF) and reverse-osmosis (RO) are the types of membrane processes used in wastewater treatment. These are pressure driven processes. The separation and typical permeate flux ranges for three important filtration types based on asymmetric porous structures are given in Table 3.1.

Table 3.1. Classification of membrane processes.

Membrane Process	**Separation Range**	**Flux Range** $L.m^{-2}.h^{-1}.bar^{-1}$
Microfiltration	10μm-100nm	>50
Ultrafiltration	10-100nm	10-50
Nanofiltration	1-10nm	1.4-12

Porous membrane filtration mechanism is based on particle size, particle charge and specific chemical interactions (Guillen and Hoek, 2010). The particles that are held internally by the membrane structure and soluble substances cause the reduction of the membrane permeability. This mostly leads to irreversible clogging. Dominant filtration/separation mechanism is based on particle/species size which is schematically illustrated in Figure 3.1. If the particle size is smaller than pore size, particles can pass

through the membrane. Particles with sizes larger than the pore size are rejected by the membrane. The pore size and its morphology may have a distribution in an asymmetric membrane.

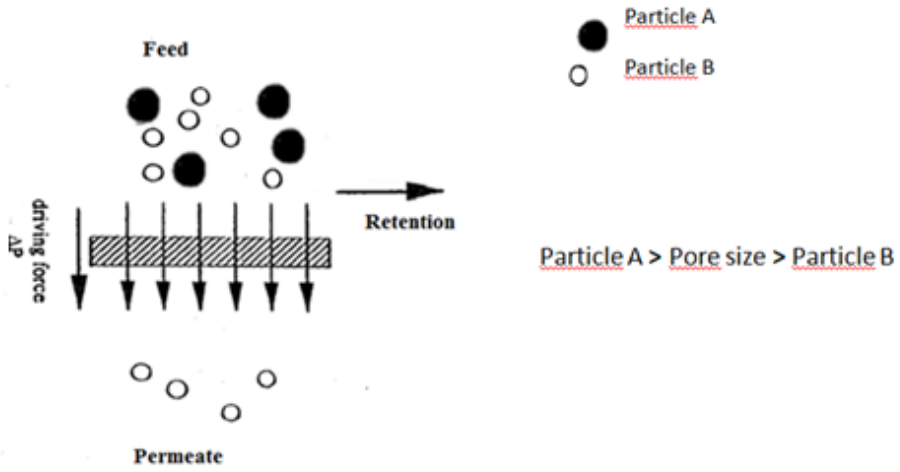

Figure 3.1. Separation mechanism of membrane.

The solute might be amphoteric or amphiphilic and can change shape when forced to pass through the membrane pores. In Ferry model, which was developed to explain the mechanism of granular filtration, particles have been shown to be rejected mainly by pore structure based exclusion. This model however does not take into account the membrane-particle interfacial forces. The solute/membrane surface chemistry and sometimes the chemistry of the feed water affects chemical exclusion. A temporary polarization occurs as a result of unequal load distribution due to the constant movement of the electrons between two species or permanent dipoles. Solutes are being pulled into the pores due to the Van der Waals forces. Van der Waals forces may also cause adsorption on the inner and outer surfaces of the membrane. Coulomb interactions between the membrane surface and particles cause the formation of a double layer by overlapping electrical layers. Compression of the electrical double layer provides a closer membrane surface approach to particles prior to effective electrostatic repulsion. If particles (less than 10 nm) approach closer to the membrane surface, short-range non-specific and specific interactions activate. Hydrophilic particles can be excluded by the pores of the membrane or membrane surface due to adhesion of particles on membrane surface. Particles can also be excluded due to the presence of a surrounding multilayer

regular water molecules. Water which is adsorbed to the hydrophilic surface is linked by strong ties and dehydration does not allow particles to adhere because it requires an enormous energy. In contrast, the hydrophobic particles which are forced by the water on the membrane surface, are trapped by the adsorption of the membrane surface. Selectivity and permeability are main factors that specify the activity of a membrane. Permeability can also be measured as the flux with L/m^{2}h units. These two factors depend on the nature of the membrane. The parameters used in the design and operation of a membrane system will be discussed as defined in Figure 3.2.

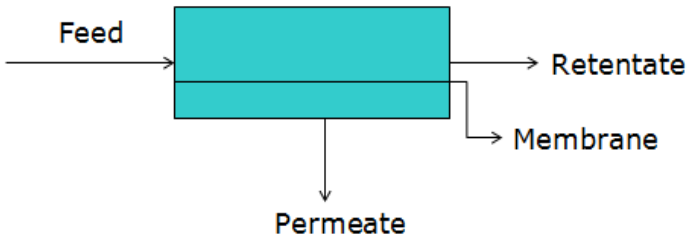

Figure 3.2. The membrane system.

Feed water: Wastewater introduced to the membrane system

Permeate: Purified water stream obtained from the membrane system

Retentate: Rejected wastewater stream

$$J_t = \frac{Q_p}{A}$$

J_t= Total flux at time t (L/m^{2}h)

Q_p= Permeate flow rate at time t (L/h)

A= Total membrane surface area (m^2)

$$J = \frac{TMP}{\mu R_T}$$

TMP= Transmembrane pressure (bar)

R_T= The total resistance to flow

μ =Dynamic viscosity (N s/m^2)

The average transmembrane pressure is calculated by the following equation:

$$TMP = \frac{(P_f + P_r)}{2} - P_p$$

P_f= Pressure on the membrane module inlet (psi)

P_r= Pressure on the membrane module exit (psi)

P_p= Permeate pressure (psi)

The total resistance of the membrane (R_T) can be considered to be formed of several resistances (Figure 3.3). The particles in the wastewater form the cake layer and are the cause of reversible or irreversible fouling.

$$R_T = R_m + R_c + R_f$$

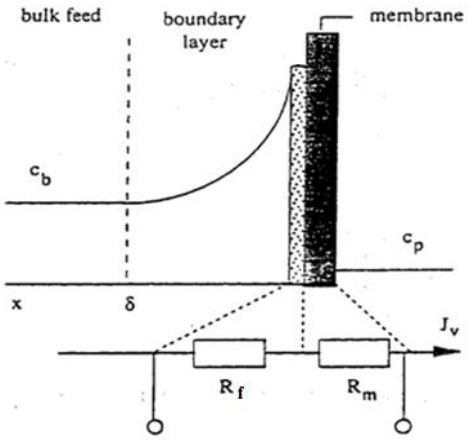

Figure 3.3. Modelling of total resistance of membrane.

J= Permeate flux

ΔP=Trans-membrane pressure

μ =Viscosity of the permeate

R_T = Total resistance

R_m = Intrinsic membrane resistance

R_c=Cake resistance formed by the cake layer (which could be removed by physical membrane cleaning mechanism)

R_f =Fouling resistance caused by solute adsorption into the membrane pore (which can be cleaned mainly by chemical cleaning operation)

Another performance factor is selectivity. Concentration difference between feed and permeate water streams is defined as selectivity of the membrane and is a

commonly used measure of performance. Selectivity is determined in percentage according to the following equation:

$$R(\%) = 100 \cdot \left(\frac{C_f - C_p}{C_f} \right) = 100 \cdot \left(1 - \frac{C_p}{C_f} \right)$$

Selectivity and flux values are important for the determination of membrane performance.

3.2 Classification of membranes

The membrane separation process is based on different driving forces. Porous membrane separation process is a pressure driven process. The advantage of pressure driven process is related with speed of the process which can be adjusted by increasing the hydraulic pressure. Microfiltration(MF), ultrafiltration(UF), nanofiltration (NF) and reverse osmosis(RO) are the four major types of pressure driven membrane processes. These membrane separation processes differ by size/molar masses(MWCO) of the separated particles/species, pressure range utilized during the filtration process and the porous/nonporous nature of the membrane (Table 3.2). The pore size of the membrane structure is the most important property in this classification. The pore size of the membrane effective in membrane filtration is called as the molecular weight cut-off (MWCO) defined in daltons (which is equal to 1g/mol). The MWCO assigned to a specific membrane is a measure of the molecular weight/size of the species which is about 90% retained by the membrane (Burgal et al. 2015).

Table 3.2. Classification of pressure driven membrane processes.

Process	Minimum particle size removed	Applied pressure	Type of membrane
Microfiltration	0.025-10 μm micro particles	0.1-5 bar	Porous
Ultrafiltration	5-100 nm macromolecules	0.5-9 bar	Porous
Nanofiltration	0.5-5 nm molecules	4-20 bar	Porous
Reverse Osmosis	< 1 nm salts	20-80 bar	Nonporous

The level of applied pressure is related with size of the target particles, properties of the liquid, and the dissolved solids content. Applied pressures in membrane processes increases from microfiltration to reverse osmosis. The decreasing pore size increases the membrane resistance to flow thus increasing the level of the applied pressure (Leslie et al. 2012).

Applied pressure varies in between 0.1 to 5 bar in microfiltration. The size of the removed particles vary in between 0.025 to 10 μm. Generally suspended solids, large colloidal particles, bacterias are removed from target liquids with microfiltration membranes. The microfiltration process is heavily applied in food/dairy industry, and biotechnology.

Ultrafiltration membranes are porous working in a pressure range of 1 to 9 bar. The size of the removed particles lies in between 5 to 100 nm. Ultrafiltration is a purification process where macromolecules and colloidal particles are removed. Common applications of ultrafiltration are in the separation of proteins and purification streams in food industries.

Nanofiltration based separations are between ultrafiltration and reverse osmosis processes. Nanofiltration process works at relatively high pressures in the 4 to 20 bar range. Relatively small species/molecules of about 1nm in size and some salts are removed in these nanofiltration applications. Monovalent salts are removed up to 20-80% and divalent salts up to 90-97% (Damas et al.2012) in nanofiltration which is commonly used in desalination and wastewater treatments.

Dissolved salts and ions can be successfully removed by reverse osmosis membranes. This process provides high removal efficiencies in the treatment of effluents from chemical, textile, pulp and paper, petroleum industries. Nanofiltration processes work at high pressures in the 20 to 80 bar range.

3.3. Materials used in membrane preparation

3.3.1 Polymeric organic membranes

Polymeric membranes are commonly used in separation processes in the industry currently. Organic membranes are prepared by using polymerization or copolymerization processes. The flux, separation and separative capacity is related with

the nature of the polymeric structures and chains, membrane morphology, and its preparation method. Polymeric membrane structures can be classified in four groups as polyethylene with a long chain , polybutadiene with a branched chain, phenol formaldehyde having a three-dimensional highly crosslinked structure, an butyl rubber with a moderately crosslinked structure (Nunes et al. 2010). The polymeric structure and the state of aggregation of the macromolecules effects the crystallinity, pore size distribution and density of the membrane which may effect the mass transport through the structura and the mechanical properties significantly.

3.3.2 Inorganic membranes

The inorganic membranes are divided into four groups as ceramic, glass, zeolithic and metallic membranes. Inorganic materials are relatively more resistant to acidic or corrosive solutions, and high temperatures compared to their polymeric counterparts. Although polymeric membranes can be used in between 90-340^{o}C, ceramic membranes can be used at 800^{o}C. (Lin et al. 2001). The level of this application temperature of inorganic membranes is related with processing and the chemical nature. The pore size and its distribution along with mechanical properties can be controlled the heat treatment stage of membrane preparation.

3.3.2.1. Advantages of inorganic membranes

Polymeric membranes dominate the membrane market currently and inorganic membranes are used in specific applications where polymeric membranes cannot be used. The polymeric membranes are not durable to organic solvents. High temperature can also damage the polymeric membrane. It is not suitable for many acidic and caustic solutions. Therefore the use of polymeric membranes is limited in many applications.

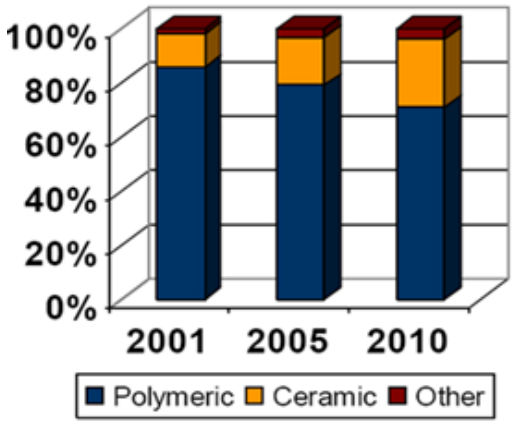

Figure 3.4. Market share of polymeric, ceramic and other material membranes. (Source: Benko et al. 2012)

Market share of inorganic membranes is increasing year by year as shown in Figure 3.4 (Benko et al. 2012). The increasing market share of ceramic membranes is related with the improvements in their molecular weight cut-off values, chemical/thermal resistance, their significantly longer lifetime and their superior mechanical properties as outlined for nanofiltration membranes in Table 3.3. These ceramic membrane related advantages can be realized with commonly used oxide materials like alumina, zirconia, silica and titania.

The ceramic membranes are currently used in industries such as food processing, beverage production, chemical manufacturing, biotechnology and wastewater treatment. Purification of wastewater by using ceramic membranes may be used towards drinking water production in the near future. The application of ceramic membranes is currently limited to microfiltration and ultrafiltration for drinking water treatment. Contaminants and trace organic chemicals (TOC) with molecular weights in the 200-300 Da range present in wastewater are removed by polymeric nanofiltration (NF) membranes towards drinking water production (Capar et al. 2008)

Table 3.3. Comparison between ceramic and polymeric nanofiltration membranes.

Properties	Ceramic Nanofiltration	Polymeric Nanofiltration
Cut-off	Down to 450 Da	Down to 200 Da
Chemical Resistance	Very Good	Acceptable
Thermal Resistance	Very Good	Acceptable
Flux (l/m^2h bar)	Good	Acceptable-good
Cleanability	Very good	Acceptable
Pricing	Acceptable	Good

Ceramic membranes are preferable for water quality management. High quality drinking water can be obtained by using ceramic membranes. Ceramic membranes with relatively large pore sizes (MWCO >500 Da) were successfully produced in the last 10-20 years but recent investigations indicate the possibility of the commercial production of ceramic NF membranes with even smaller pore sizes (MWCO = 200 Da) (Li et. al. 2011). The main disadvantage of ceramic membranes is their relatively higher initial cost. However, the lifetime of ceramic membranes is longer than polymeric membranes. The cost of ceramic membranes has been decreased in the last years by new investigations and applying new technologies (Damas et al. 2012).

3.4 Challanges of membrane technology

3.4.1 Fouling

The permeate flux decreases with time approaching to a limiting flux due to concentration polarization, fouling and adsorption of molecular species on the membrane surface as schematically shown in Figure 3.5. This permeate flux decrease is closely related with the properties of the membrane surface and the feed wastewater characteristics (Angelis et al. 2013).

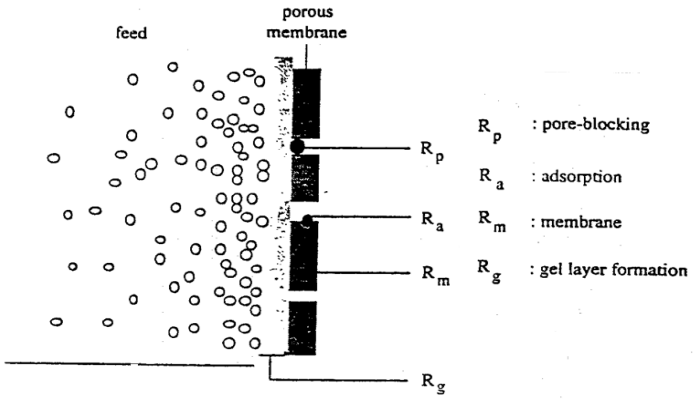

Figure 3.5. The schematic presentation of membrane fouling and corresponding membrane resistance components.

The total membrane resistance to permeate flux is formed from four resistance components. The first of these components is known as the membrane resistance R_m which is the resistance to water flow free of contaminants. Concentration polarization resistance R_{cp} , gel layer resistance R_g and surface adsorption related resistance R_a combined form the commonly known fouling resistance. Gel layer resistance is due to the formation of a gel layer with increasing concentration of species/salt close to the membrane surface. The pore blocking resistance (R_p) develops during filtration due to the blocking of the membrane pores by the entraped particles/species. Adsorption resistance R_a is related with chemical species adsorption on the membrane pore surfaces. Membrane fouling mechanisms are schematically shown in Figure 3.6.

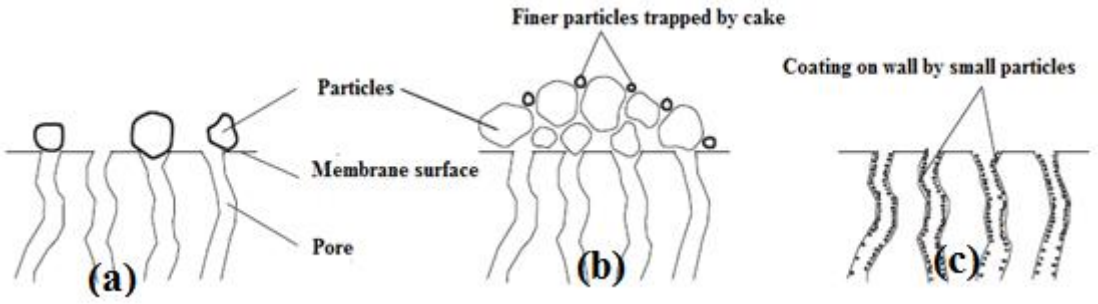

Figure 3.6. Membrane fouling mechanisms: (a)particle rejection, (b)cake filtration and (c)particle adsorption.

.

Membrane fouling can be minimized by proper membrane selection, module type, operation conditions and chemical/physical cleaning. Membrane fouling

minimization strategy must include the proper choice of the feed solution with a low fouling tendency and a hydrophilic membrane choice for water based feeds. Crossflow filtration is preferred to dead end filtration (Fan et al. 2001). Cross flow filtration forms turbulant flow where fouling on the membrane surface is minimized with the nature of the flow.

3.4.2 Concentration polarization

The solute concentration in the permeate is less than the solute concentration in the feed during membrane filtration through the retention of the solute and the preferential permeation of the solvent. The concentration of the retained species on the membrane surface increases during the filtration and their concentration becomes more than that of the feed causing concentration polarization. The difference of the species concentration between the feed and the permeate streams causes the formation of a concentration gradient at both sides of the membrane (Macedo et al. 2011). The retained molecules can diffuse back to the bulk of the feed as a result of this concentration gradient. Permeate flux through the membrane and back diffusion of solutes which to the bulk retentate stream from the boudary close to the membrane surface feed will come to a steady state condition in time.

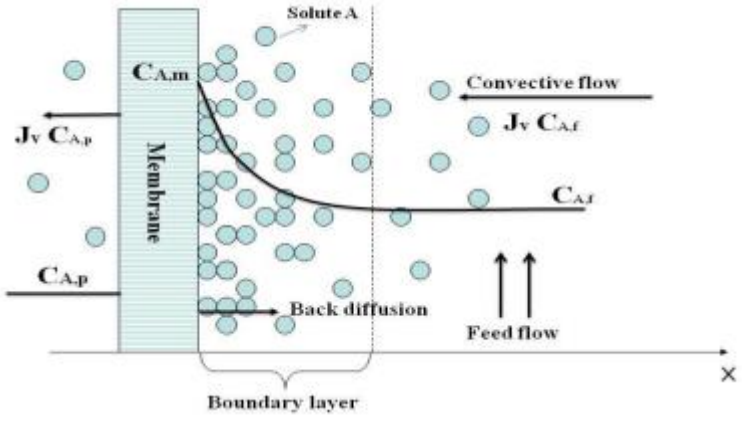

Figure 3.7. Concentration polarization phenomenon.

Concentration polarization is descibed by the formation of a thin of the unmixed solution between the membrane and the bulk of the well mixed feed film which is called as the boundary layer as shown in Figure 3.7. The solute concentration of the bulk is

$C_{A.f}$ at distances higher than the boundary layer thickness (d) and close to the membrane surface the concentration increases in the boundary layer to a maximum of $C_{A,m}$ and the convective transport of the solute toward the membrane is given by the following equation :

$$J_v c_i = J_v c_{ip} + D_i \frac{dci}{dx}$$

Jv is the volumetric flux in the boundary layer, Cip is the concentration of ion (*i*) in the permeate and Di is the diffusion coefficient of ion(i).

CHAPTER 4

CERAMIC MEMBRANES AND HISTORY

Ceramic membranes are first produced lab scale in the 1940s. The pioneering large scale application of ceramic membranes were towards uranium enrichment through gaseous diffusion in porous membranes. The uranium concentration and enrichment application in the nuclear industry has been used for over 25 years with modified ceramic membranes. The R&D efforts on ceramic membranes began again in the 1970s. Micro/ultrafiltration ceramic membranes were developed and used in separation processes in food/dairy industries. The water treatment, food and chemical industries started using ceramic membranes in their separation processes. Many producers in Europe were involved in the production of ceramic membranes since the chemical and mechanical properties of ceramic membranes were superior to polymeric membranes. Commercial porous ceramic membranes in different geometries(single or multi-channel tubular) contaning thin selective ceramic layers became available shortly after these years. Ceramic nanofiltration membrane MWCO values were about 350 Dalton in those years. Ceramic ultrafiltration and nanofiltration membrane performances are coming even more closer to reverse osmosis membranes currently.

4.1 Preparation of selective layers

4.1.1 Microfiltration layer

Selective layers are prepared by using ceramic powders several microns in size and even a larger size distribution formed from particles with different morphologies. The preparation processes, materials and pore diameters of the selective layers present in inorganic membranes along with their chemical differences are tabulated in Table 4.1

Table 4.1. Inorganic membranes; preparation process, materials and pore diameter. (Tsuru, 2008)

Type	Preparation Process	Materials	Pore Size
Porous Membrane	Powder sintering	Al_2O_3,ZrO_2,TiO_2	100nm
	Sol-gel	SiO_2,Al_2O_3,ZrO_2,TiO_2	1-50nm
	Phase separation	SiO_2	4nm
	CVD	SiO_2	<1nm
Non-Porous Membrane	Inorganic-Organic Composite	Al_2O_3/MgO,Ag	
	Metal	Pd,Pd/Ag	

The pore size in microfiltration membranes is commonly larger than 100 nm. Alumina is the most commonly used material for microfiltration layer preparation. Zirconia, titania and silica powders may also be chosen for specific applictions. ZrO_2 and α-alumina powders was used for the formation of microfiltration layers in oil-water and aquatic contaminants separations (Yang et al. 1998). Alumina, zirconia, titania have high production cost. These materials are used for high separation performance processes which are biochemical, bioprocessing and casein from whey protein separation applications (Ivanets et al. 2014). Low cost applications of microfiltration membranes are based on kaolin, sodium carbonate, boric acid and quartz. Kaolin is the most commonly used material for low cost applications. Stability and cost is more preferable than other materials (Potdar et al. 2002).

Microfiltration layers can be formed by preparing a suspension of inorganic particles and depositing inorganic particles on porous support surfaces by slip casting method. The most important suspension preparation parameters are the viscosity, dispersant and binder content, solids content. Milling and/or ultrasonification are usually applied for the deagglomeration of the powders. Dispersant provides preparation of well dispersed suspensions necessary for the preparation of homogenous defect-free microfiltration layers. Optimum amount of dispersant can be determined by considering the total surface area of the powder. Excessive amounts of organic additives/binders are undesireble in the preparation of the suspension. Binder/organics removal during successive heat treatment of the selective layer may form large defects in the structure of the microfiltration layer.

Solids content is an important parameter in the suspension casting of microfiltration layers. Increasing the solid content may cause air bubble generated defects and pinhole formation on the microfiltration layer surface. The air bubbles can be removed by using defoamer addition and the vacuum deairing of the suspension.

Surface roughness is a serious problem which causes colloidal fouling during the use of microfiltration membranes. The AFM pictures given by Vrijenhoek indicated that more particles were deposited on the rough surfaces of the microfiltration membrane. The particles preferred ‘valleys’ which caused valley clogging during filtration. The use of polyvinylalcohol for the modification of suspension viscosity and flocculation along with the use of 0.5 micron powder particle size were concluded to be beneficial for the reduction of surface roughness (Vrijenhoek et al. 2001). The use of dispersant prevented flocculation and significantly reduced the selective layer surface roughness (Zhong et al. 2012).

4.1.2 Ultrafiltration Layer

The pore size of ultrafiltration membranes are in the 2-100 nm range(Tsuru, 2008). Ultrafiltration membranes are used in the separation of whey protein concentrate, wastewater treatment, removal of pathogens from milk, and removal of iron salts from water (Fersi et al. 2009).

Boehmite, zeolites, carbon, ceramic oxides such as zirconia, titania are commonly used for the formation of ultrafiltration selective layers. High performance ultrafiltration formed from zirconia, titania, zirconia/boehmite and titania/boehmite selective layers are commercially available (Yang et al. 1998). The pioneering ultrafiltration membrane was prepared by using zirconia/boehmite sol composites (pore size 20-100 nm) and was commercialized by membralox company in 1988. Several companies commercialised their ultrafiltration membranes as given in Table 4.2.

Table 4.2. Commercialized ceramic membranes.

	Filtration Range	Support Materials	Membrane Materials
Pall	5nm to 2μm	Al_2O_3	Al_2O_3(MF),ZrO_2,TiO_2(UF)
Corning	5nm to 2μm	Mullite	ZrO_2(MF) ,TiO_2(UF)
Tami	0.02μm to 1.4μm	ATZ	ZrO_2(MF) ,TiO_2(UF)
Atech	0.01μm to 1.2μm	Al_2O_3	Al_2O_3(MF),ZrO_2,TiO_2(UF)
Orelis	5kDa to 0.8μm	Al_2O_3	ZrO_2 and TiO_2

Preparation of ceramic oxide membranes or layers can be performed by sol-gel method. The formation of a membrane pore structure with fine interconnected uniform pores can be easily accomplished by using sol-gel processing. Sol-gel method was developed by Yoldas in 1975. Aluminum alkoxide was hydrolyzed at 85^{o}C with 2 L of water per mole of the alkoxide. The suspension was further peptized with 0.07 moles of HNO_3 per mole of alkoxide.

Sol-gel processing precursor chemicals are metal salts or alkoxides. Preparation of a stable sol includes two simultaneous reactions which are hydrolysis and condensation as shown in Figure 4.1.

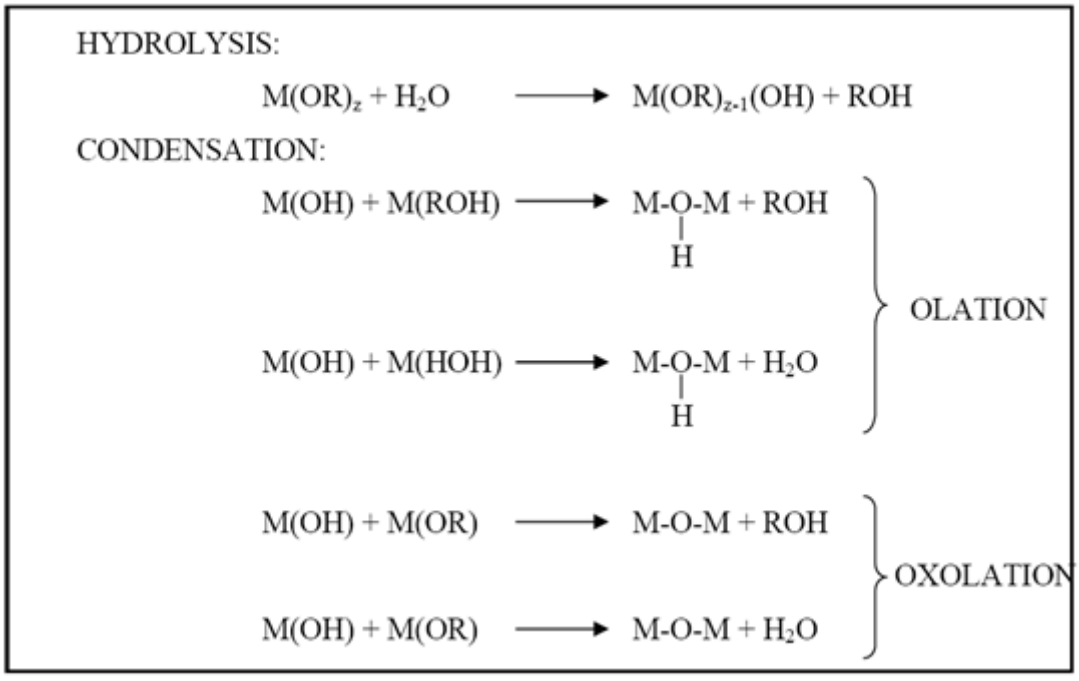

Figure 4.1. Hydrolysis and condensation reactions.

Reactive alkoxy group(-OR) of the metal alkoxide is replaced by the hydroxyl (-OH) group of a water molecule along with the formation of an alcohol molecule (ROH) in hydrolysis reaction. Number of hydroxy ligands (M-OH) and charge density of metal (M) increase the hydrolysis reaction rate. The condensation reactions include ‘olation’ or ‘oxolation’ steps and is very sensitive to the preparation atmosphere. The hydrolysis and condensation reaction rates have a significant effect on the sol particle size distribution. High condensation reaction rates cause higher nucleation rates and precipitation. The hydrolysis and condensation reaction rates may be controlled by alkoxide/solvent/catalyst type and temperature.

4.1.3 Nanofiltration Layer

The nanofiltration membranes have pore sizes in the 1- 2nm range. Zirconia and titania are the most commonly used inorganic materials for nanofiltration layer preparation. Titania and zirconia sols have good colloidal stabilities. The stability of these sols along with nanodesignable sol particle sizes may provide a close control of the pore size necessary for a specific separation application. Nanofiltration sols are prepared from pure zirconia and titania or from their composites. The nature of the sol mixture may effect the homogeneity and the properties of the final oxide nanostructure (Zeidler et al. 2014). Another nanofiltration material is amorphous silica which is prepared by hydrolsis and condensation of silicon based alkoxides. Amorphous silica provided controllability of pore size like titania and zirconia, but silica layers have a lower chemical stability. Zirconia and titania based layers are commonly used in the preparation of nanofiltration membranes due to their relatively higher chemical stability (Gestel et al. 2006). The stability of silica is improved by zirconia. The defect–free silica-zirconia nanofiltration membranes were prepared by hydrolysis and condensation reactions of tetraethoxysilane (TEOS), zirconium tetra-n-butoxide and acid catalyst (HCl) (Tsuru et al. 2000).

Nanofiltration layer is prepared by sol-gel process. The sol-gel process includes condensation and hydrolysis reactions and rate of these reactions is controlled by acid catalyst. The sol-gel process is conducted in two main routes which are polymeric and colloidal sol-gel routes. The hydrolysis and condensation reactions of colloidal sol-gel route are faster than polymeric sol route. These faster condensation reactions present

during colloidal sol preparation may cause precipitation or uncontrolled particulate growth.

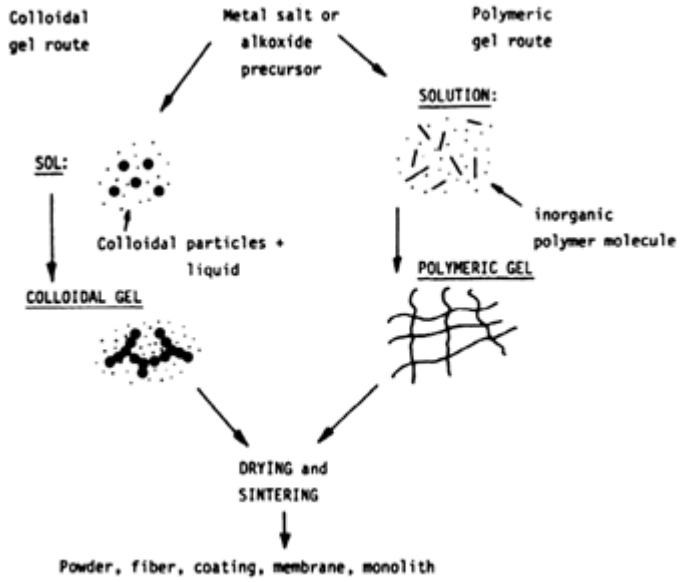

Figure 4.2. Scheme of polymeric gel route and colloidal sol-gel route.

The hydrolysis reaction rate of polymeric sol route is lower than colloidal sol route. A much smaller amount of water is used for hydrolysis of the alkoxide in alcohol in polymeric sol route which is schematically shown in Figure 4.2. Gelation occurs after complete hydrolysis-condensation reactions. Linear inorganic structures form the gel like network in polymeric sols during gelation. The size and particle packing level of polymeric and colloidal sol particles have a significant effect on membrane pore size. Membranes with relatively large pore sizes can be prepared by using colloidal sol particles since the packing factor of colloidal particles is low. The polymeric sol is convenient for the preparation of microporous structure.

Generally the preparation of nanofiltration layer is conducted by using titania sols. Many companies commercialized titania nanofiltration membranes with small pore sizes in between 1-2 nm. TTIP (titanium-isopropoxide) ,water , acid catalyst and isopropanol are used in the preparation of polymeric titania sols. The TTIP/isopropanol molar ratio and TTIP/water ratio (molar ratio Ti^{+3}/ H_2O =2.5-5) (Erdem et al. 2006) and acid catayst level all have significant effects on particle size distribution of the final polymeric sols. The zirconia sol is prepared by using zirconium isopropoxide in propanol. Increasing amount of nitric acid in the zirconia sol decreased the particle size from 5.2 nm to 3.1 nm (Erdem et al. 2006). On the other hand, an excessive amount of nitric acid in the sol causes the agglomeration of the nanosized sol particles. The

presence of large agglomerates creates irregular packing particle in the top layer which furter causes microcracks during drying/heat treatment.

The thickness and the drying/heat treatment conditions of the nanofiltration top layers also are very important for the preparation of defect-free selective membrane layers. The viscosity of the precursor sols, formation of relatively thick nanofiltration layers and their rapid rate of drying/heat treatment can be the major reasons behind the crack/defect formation in the top nanofiltration layer surfaces. The polyvinyl alcohol (PVA) and diethanol amine (DEA) addition to the sols may contribute to the sol viscosity improvement and drying control.

CHAPTER 5

APPLICATION OF MEMBRANE SEPARATIONS FOR TEXTILE WASTEWATER TREATMENT

The textile industry is the biggest consumer of dyes, chemical compounds and uses huge amounts of water. The textile industry consumes about 0.3 m^3 of water per kg textile production (DSI, 2012). The dying, printing, finishing and washing operations in textile procesing consumes this large level of water. The chemical content of textile wastewater depends on the nature of the finishing operations, equipments and the chemical and physical characteristics of dyes. The properties of wastewater is important in membrane performance assesment during treatment/purification applications.

The microfiltration membrane application is limited in textile wastewater treatment. Colloidal dyes and particles may only be removed by microfiltration (Van der Bruggen et al. 2004). The performances of flocculation, nanofiltration and microfiltration membrane filtration processes were compared in a recent work. The flux of nanofiltration membranes were deterined to increase from 8L/m^2h to 15L/m^2h when microfiltration membrane was used as a pretreatment in textile wastewater recovery. Microfiltration considerably reduced COD, color, turbidity and also fouling of the nanofiltration membranes (Ellouze et al. 2012).

Ultrafiltration membranes are used in the removal of colloidal macromolecules with a few thousand dalton in molecular. Application of ultrafiltration membranes are limited in textile wastewater treatment. Ultrafiltration is not efficient for prior step of wastewater treatment. Ultrafiltration is kind of a pretreatment for reverse osmosis and nanofiltration (Damas et al. 2010).

Ultrafiltration membranes are commonly used in the axuiliary treatments like washing, flushing and softening processes in textile industry. The 20,50,150 kDa molecular weight cut off ceramic ultrafiltration membranes were used in textile wastewater pretreatment. Significant reductions in chemical oxygen demand (>70%), color (96%) and turbidity (>93%) were obtained with ceramic ultrafiltration membranes. These results show that the ceramic ultrafiltration membranes can be

efficiently used as a suitable pre-treatment process for further nanofiltration and reverse osmosis applications (Damas et al. 2010).

The textile wastewater was collected from reclaimation of dye bath (pH is between 5.0-6).The performance of nanofiltration membranes was investigated with three different treatment stiuation. First one; single nanofiltration with pH neutralization, second; single nanofiltration without pH neutralization, third; microfiltration is use kind of pre treatment with nanofiltration and pH neutralization. The best treatment was nanofiltration with pretreatment and pH neutralization (Capar et al. 2006).

CHAPTER 6

EXPERIMENTAL

6.1. Materials

The materials used in experimental work are given Table 6.1. The textile wastewater was supplied by Sun Tekstil, İzmir, Türkiye.

Table 6.1. The materials used in experimental work.

Materials	Property
Alumina Powder Al_2O_3	High purity ALMATIS CT 3000 SG
Ethanol	High purity FW: 46.7, d: 0.81, Merck
Nitric Acid, HNO_3	65% FW: 63.01, d: 1.4, Aldrich
Polyvinyl alcohol,PVA	80% hydrolysed, MW: 9000-10000, Aldrich
Boehmite Powder AlO(OH)	High purity acid dispersible Disperal, Sasol
1-Propanol	High purity, FW:60.10, d:0.8 ,Riedel
Titanium (IV) isopropoxide	97 %, Aldrich
Diethanolamin	Merck
Dolapix CE 64	Eurokimya A.Ş
Defoamer	Dağlar Kimya A.Ş

6.2.Method

The tubular alumina supports were dip-coated with α-alumina, boehmite and titania sol. The tubular ceramic membranes were coated with two intermediate layers and a thin top layer. The asymmetric membrane structure with graded pore sizes is illustrated schematically in Figure 6.1.

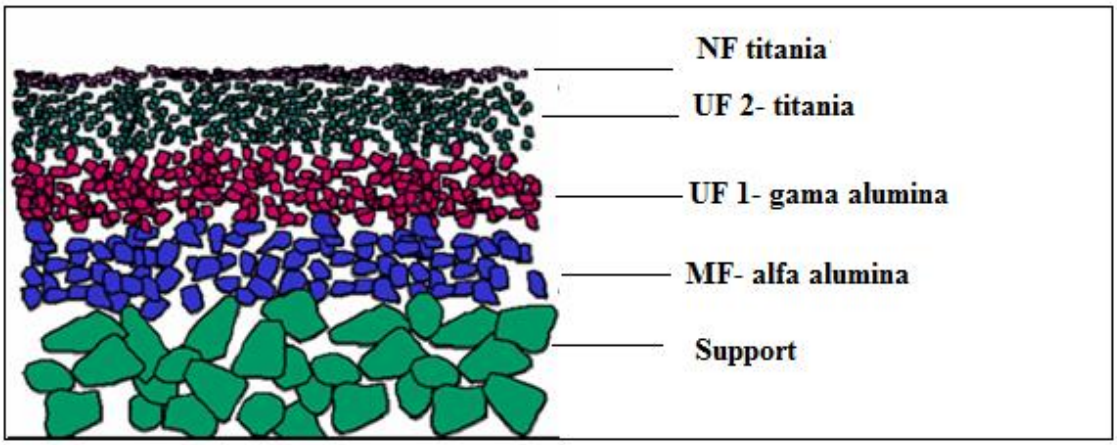

Figure 6.1. The layers of the asymmetric ceramic tubular membrane.

In this study α-alumina powders with different particle sizes/surface areas were used. Alumina supports were produced from a mixture of α-alumina powders with different particle sizes (0.5, 1.3, 4, 5.2 μm average size). Microfiltration layer was prepared by using a stable suspension of 0.5μm α-alumina.

α-alumina powders were characterized by scanning electron microscope (SEM) (FEI QUANTA 250 FEG), particle size distribution analyser (Micromeritics Sedigraph 5100), and X-ray diffraction (Philips X'pert pro XRD). Boehmite powders were also characterized by SEM and XRD.

Selective microfiltration and ultrafiltration layers were prepared by α-alumina and boehmite colloidal suspensions. The selective top layer was prepared by nano titania particles which were synthesized by sol-gel based polymeric sols and colloidal hydrosols. The particles sizes of the sols were determined by Zetasizer-DLS. The prepared sols were coated by a slip casting method. The sols were dried and micro and nano structures were investigated with SEM and the phase structures were characterized with XRD. The coated membrane surface images were obtained by optical microscopy (Olympus BX60M). The ceramic membrane clean water permeabilities and separation performances were determined by using a filtration set-up. The wastewater and permeate properties were determined by Hach Lange spectrophotometer.

6.3. Preparation of Selective Layers

The microfiltration layer was formed by using a stable colloidal sol with 7 wt % 0,5μm α-alumina and 1wt % PVA (M_w= 9000-10000) binder/drying control additive

contents. A commercial dispersant (Dolapix) and also a commercial defomer was also added for the preparation of an air bubble stable suspension for improving the particle packing in the slip cast microfiltration layer. The powder suspension was dispersed and deagglomerated by ultrasonic treatment in a bath for about couple of hours. PVA was used as a drying controll chemical additive (DCCA) for the preparation of crack-free selective layers.

The particle size and distribution of α-alumina suspensions were determined by dynamic light scattering (DLS Malvern Zetasizer 3000 HSA). The support was coated with α-alumina suspension for about 7 minutes. The alumina coated support was dried at room temperature for one day. The dried α-alumina coated support was heat treated at 1200^{o}C in a temperature/heat rate programmable muffle furnace (Carbolite CWF 1300). The furnace was heated from room temperature to 1000°C with 2.6°C/min heating rate, heated from 1000°C to 1200^{o}C with 2^{o}C /min heating rate, and finally it was soaked about 60 min at 1200^{o}C.

UF1 layer was prepared from boehmite sol as schematically shown in Figure 6.2. The water based boehmite sol had 2 wt% boehmite and 0.66 wt% PVA (total sol volume about 100 ml) content. This sol was peptized with 6ml 1M HNO_3 addition. Nitric acid was added dropwise to the suspension in order to avoid rapid local pH variations and gelation. Boehmite powders were dispersed/peptized by magnetic stirring for about 1 hours followed by an additional 1 hour treatment in an ultrasonic bath.

The particle size and distribution of the boehmite sol was determined by Zetasizer-DLS. The microfiltration layer was coated with boehmite sol for about 15 seconds. The boehmite coated microfiltration layer was dried at room temperature for one day. The dried boehmite coated membrane was heat treated at 600^{o}C in the furnace. The furnace was heated from room temperature to 200°C with 1.6°C/min heating rate, heated from 200°C to 400^{o}C with 1^{o}C /min heating rate and heated from 400°C to 600 ^{o}C with 1.6^{o}C /min heating rate and finally it was soaked about 60 min at 600^{o}C.

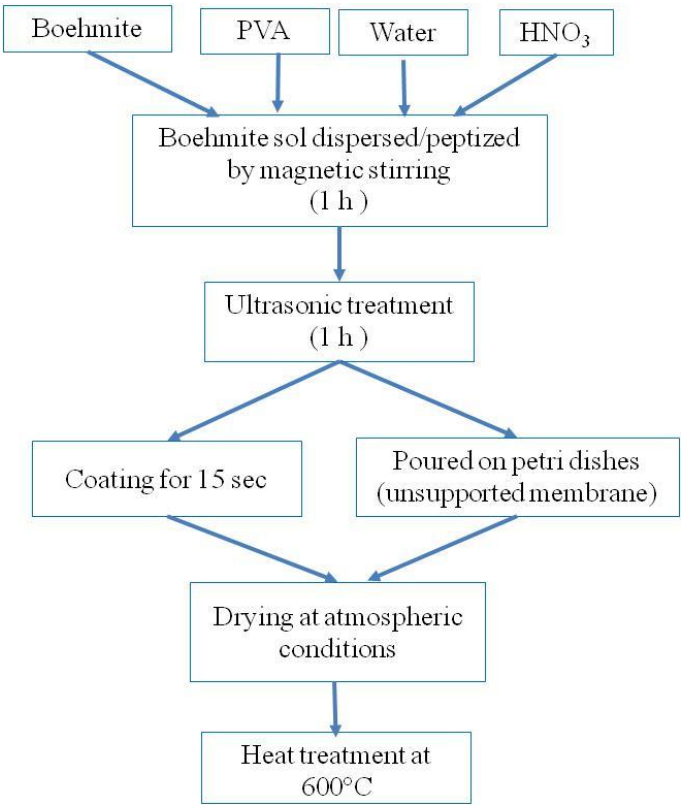

Figure 6.2. Schmatic representation of preparation of UF1 layer.

UF2 layer was formed by using a TiO_2 hydrosol as shown in Figure 6.3. Titanium IV isopropoxide, isopropanol, and diethanolamine was mixed for about 1 hour in the first stage of the TiO_2 hydrosol preparation. This well mixed solution was added dropwise to water at 45^{o}C under vigorous stirring and further mixed for an additional 1 hour. The final step involved HNO_3 addition for peptization. The molar composition of the titania sol was set as 1:0.4:2.4:1000:10 (TTIP:DEA:HNO_3:H_2O:Propanol). UF1 membrane was coated with the prepared titania hydrosol for about 10 seconds. The coated selective layer was dried at room temperature for one day. The dried UF2 layer was finally heat treated at 400^{o}C in the furnace with 1^{o}C/min heating rate and a 60 minutes soak at 400^{o}C.

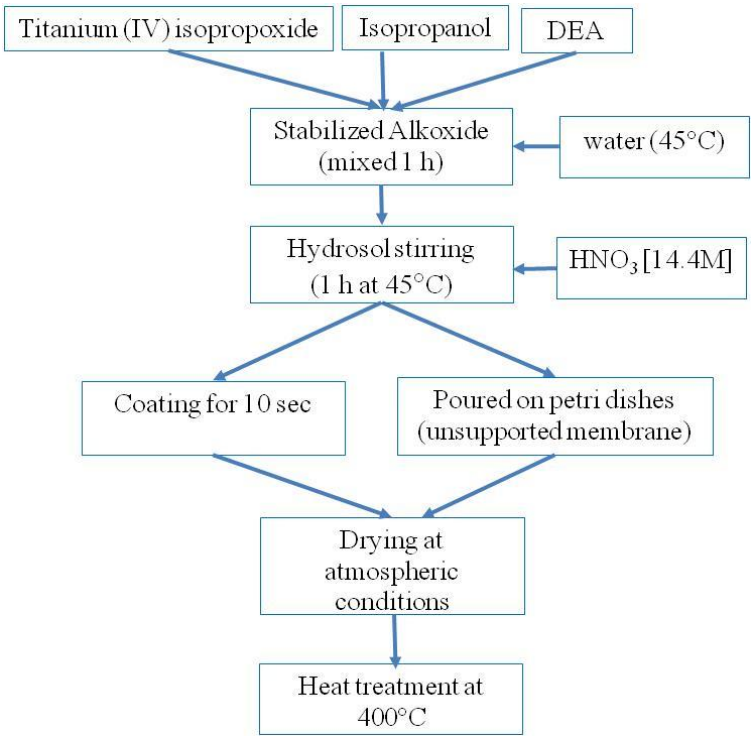

Figure 6.3. Schematic representation of UF2 layer preparation.

NF layer was prepared by polymeric titania sol as shown in Figure 6.4. The molar ratios of the sol was set as 1:0.057:2:52 (TTIP:HNO_3:H_2O:ETOH). The predetermined amounts of ethanol, HNO_3 and water were mixed 15 minutes for the formation of the water containing alcoholic solution. Similarly predetermined amounts of titanium IV isopropoxide and ethanol were mixed for 15 minutes for the formation of the second solution. The former solution was added dropwise to the latter solution under constant stirring. UF2 selective layer was coated with the polymeric titania sol in order to form the selective NF layer. The particle size distribution of the polymeric titania sol was determined by Zetasizer-DLS. The polymeric titania sol was coated for about 2 minutes and further dryed one day under atmospheric conditions. The dried NF layer was further heat treated to 400^{o}C with a heating rate 1^{o}C/min and soaked 60 minutes at the peak temperature.

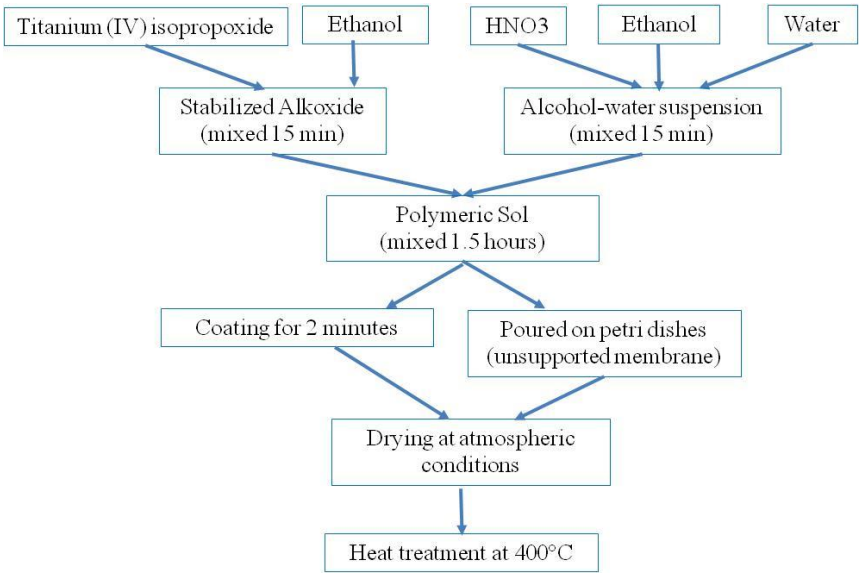

Figure 6.4. Schmatic representation of preparation of NF layer.

6.3.1 Thermal Behaviour of Selective Layer

The heat treatment schedule is very important for the preparation of defect-free selective layers with high separation performance. The most important parameters are the heat treatment temperature and the heating rate. The shrinkage/densification behaviour of the unsupported selective layers were investigated by Linzeis L76150B-1600 dilatometer. The 0.5 micron alumina suspension (MF), boehmite sol(UF1) and titania hyrosol (UF2) were dried in petri disches at room temperature. Pellets were prepared from these dried unsupported membranes by uniaxial pressing by using a laboratory dry press. The shrinkage/densification curves (shrinkage vs temperature) were obtained by conducting dilatometry runs up to 850-1300^{o}C.

6.4. Filtration Experiments

The filtration experiments were conducted on the cross flow fitration set-up shown in Figure 6.5. These experiments were conducted at room temperature. The flow in the system can be varied through the pressure pump and the pressure was adjusted by using the needle valves. Filtration experiments were carried at TMP values less than 25 bars. Membrane module and pressure pump are the most important parts of the experimental set-up. The tubular membrane module was made of stainless steel

construction and includes two membrane holding flanges at both sides of the module as shown in Figure 6.6. The cylindrical rubber 'O' rings prevent leakage of water under high pressure.

The wastewater was supplied by Sun Tekstil. The location and dates of the received textile wastewaters are given in Table 6.2. The TOC, TSS, color, pH, and conductivity of the received wastewater samples were characterized by standard methods. The pH and conductivity were measured by a portable device (Hach Lange). TOC, TSS, Color were measured by Hach Lange Dr 3900 spectrometer. Pt-Co values were measured at two different wavelengths (455 and 465 nm). Other color parameters were measured by Admi method in m^{-1} units. In this method three different wavelengths (435, 525 and 620nm) were used. The suspended solids of the wastewaters were measured at 810 nm.

Table 6.2. The locations and dates of the received textile wastewater samples from Sun Tekstil.

Wastewater No	**Collected Stream**	**Date**
1	Before biological treatment	July 2015
2	After biological treatment	November 2015
3	Before biological treatment	November 2015

The wastewater 1 was prefiltered by using a buchner funnel. The similar pretreatment was conducted by using the uncoated tubular alumina supports in the filtration set-up for wastewaters 2 and 3. These wastewaters were fed to the system in the sequential MF, UF1 and UF2 coated membrane filtration runs. Clean water fluxes were measured at different TMP's for supports, MF, UF1, UF2, and NF membranes.

Textile wastewater filtration experiments were conducted under constant pressure (4 bar) in order to analyse the flux decline during the MF, UF1, UF2 and NF membrane filtration experiments. Feed, permeate, and retentate samples were collected for analysis during the filtration experiments. The variation of the TOC, TSS, color, conductivities of feed, permeate and the retentate samples during the filtration run were determined.

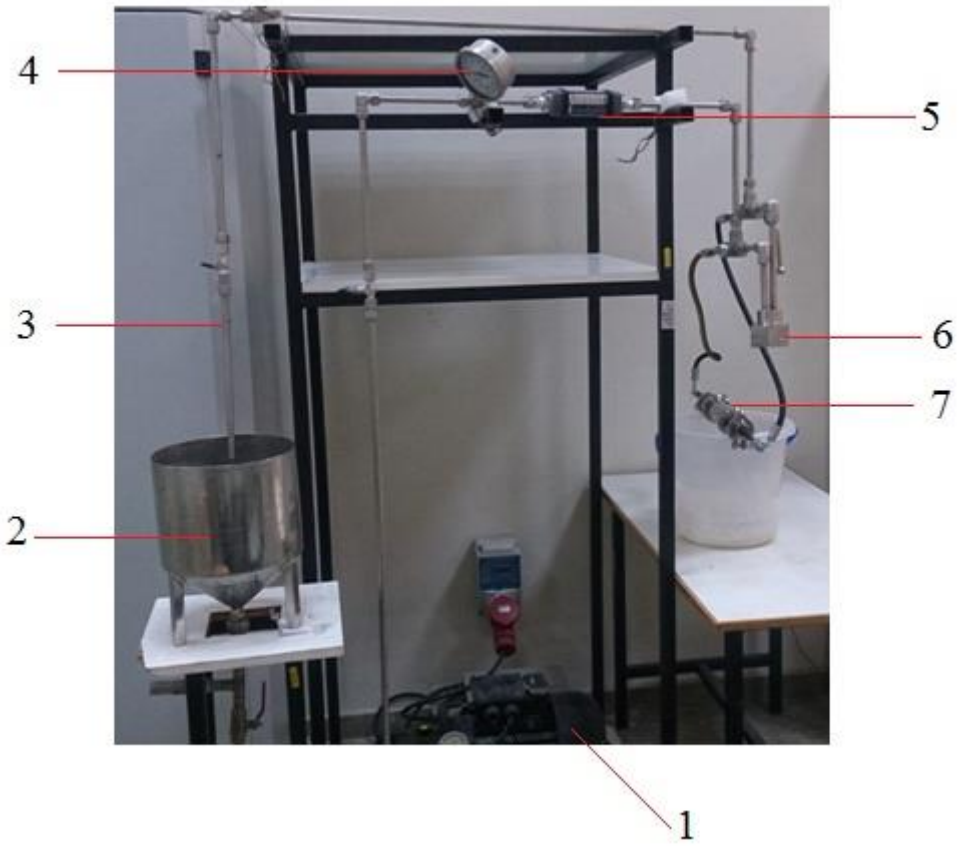

Figure 6.5 Cross flow and dead end filtration set-up; 1-pump, 2-feed tank, 3-recycle, 4-gauge, 5-flowmeter, 6-dead end cell, 7-cross-flow membrane module.

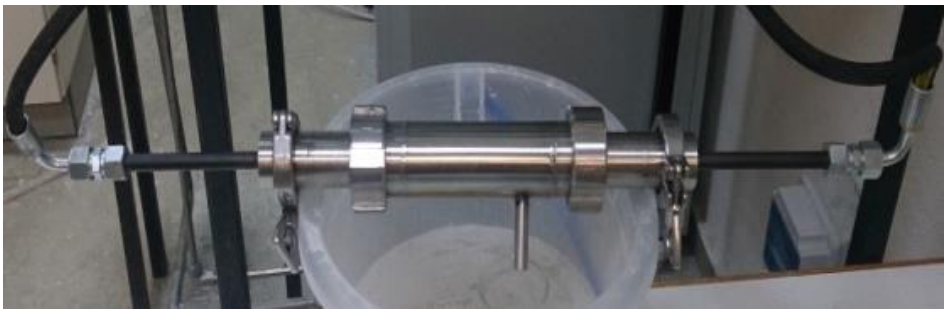

Figure 6.6. The tubular membrane module.

Membrane flux declines during textile wastewater and clean water filtration were analysed. Clean water flux of fresh membrane was defined as J_{cwi} (L/m^2h). Textile wastewater flux of membrane was defined as J_{ww} (L/m^2h). The clean water fluxes of the fouled membranes during textile wastewater filtration was determined and was defined as J_{cwf} (L/m^2h). The fouled membrane was cleaned and its clean water flux was

determined to obtain J_{cwc} (L/m^2h). The flux decline analysis were conducted based on the equations given in Table 6.3.

Table 6.3. The flux decline analysis equations.

Formula	Type/cause of flux decline
$\frac{J_{cwi} - J_{ww}}{J_{cwi}}$	Total
$\frac{J_{cwf} - J_{ww}}{J_{cwf}}$	Concentration Polarization
$\frac{J_{cwi} - J_{cwf}}{J_{cwi}}$	Fouling(Irreversible+reversible)
$\frac{J_{cwc} - J_{cwf}}{J_{cwc}}$	Reversible Fouling
$\frac{J_{cwi} - J_{cwc}}{J_{cwi}}$	Irreversible Fouling

CHAPTER 7
RESULTS AND DISCUSSION

7.1. Characterization of Powders

The particle sizes and the surface areas of the α-alumina powders used in tubular membrane support fabrication as reported by the supplier is tabulated in Tablo 7.1.

Table7.1. Particle sizes and surface areas of α-alumina powders reported by supplier Almatis Co.

	Unit	CL 4400 FG	CL 3000 SG	CT 1200 SG	CT 3000 SG
Particle Size/ d_{50}	**μm**	5.2	4.0	1.3	0.5
BET Surface Area	**m^2/g**	0.6	1.0	3.1	7.5

The particle size distributions of these alumina powders determined with Sedigraph 5100 are given in Figures 7.1 through 7.4. The d_{50} particle sizes were found to reasonably match to those reported by Almatis company.

The powder particle sizes and morphologies of the α-alumina powders (Almatis 0.5,1.3,4,5.2 μm) were investigated with SEM. The SEM images given in Figures 7.5-7.8 indicated that α-alumina powder particles were equiaxed and had mostly rounded edges with sizes close to those determined by the Sedigraph measurements.

Phase characterization of the alumina powders were conducted and their XRD patterns are given in Figure 7.9. These alumina powders were determined to be formed from pure α phase.

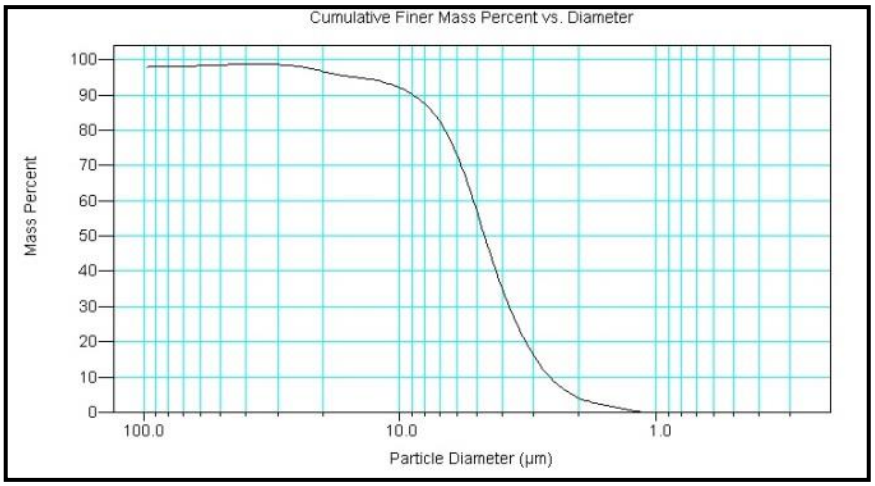

Figure 7.1. The particle size distribution of the 4 µm CL3000SG powder.

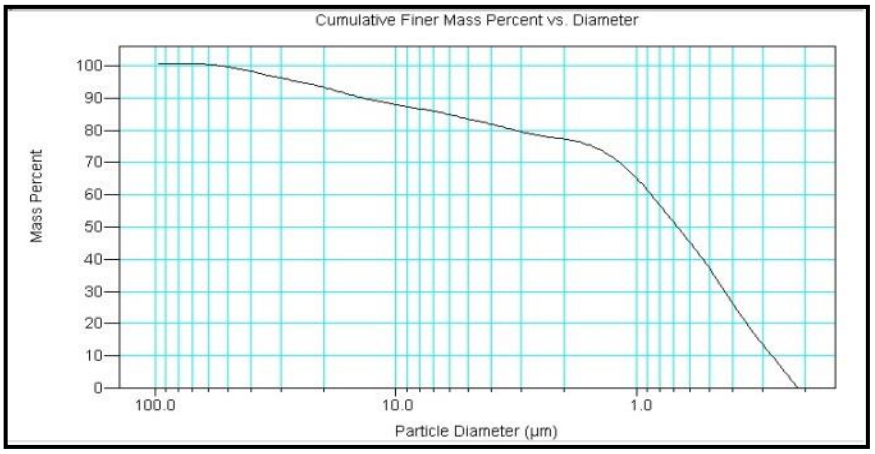

Figure 7.2. The particle size distribution of the 0.5 µm CT3000SG powder.

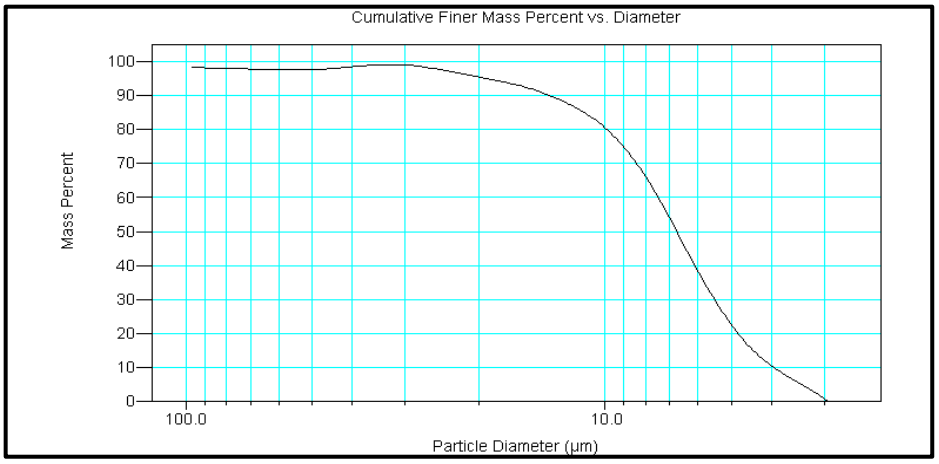

Figure 7.3. The particle size distribution of the 5.2 µm CL4400FG powder.

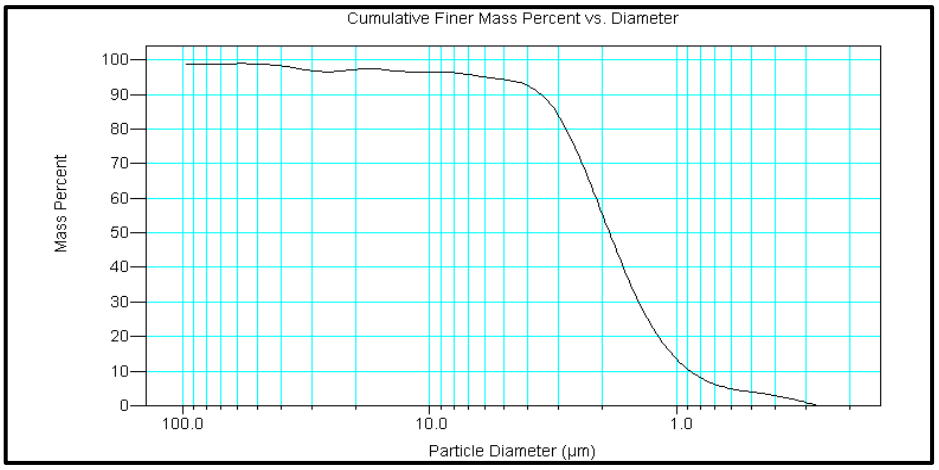

Figure 7.4. The particle size distribution of the 1.3µm CT1200SG powder.

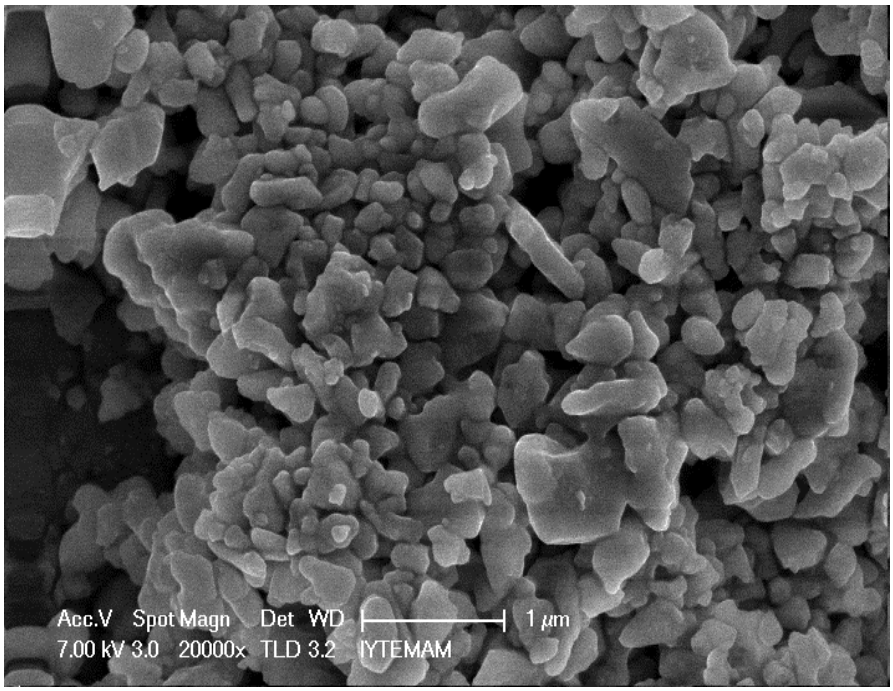

Figure 7.5. SEM image of CT 3000 SG 0.5 micron α-alumina powder.

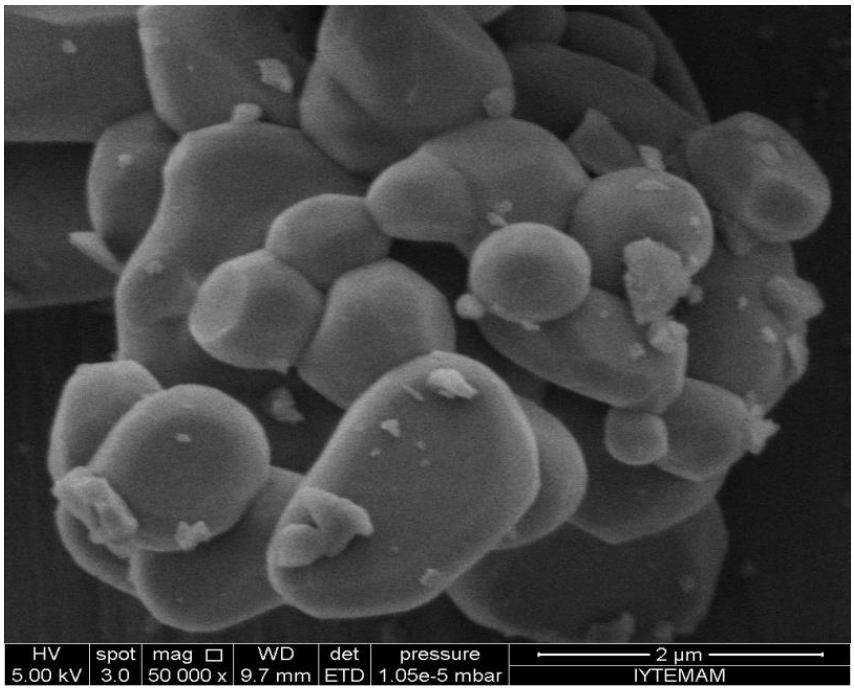

Figure 7.6. SEM image of CL 3000 SG 4 micron α-alumina powder.

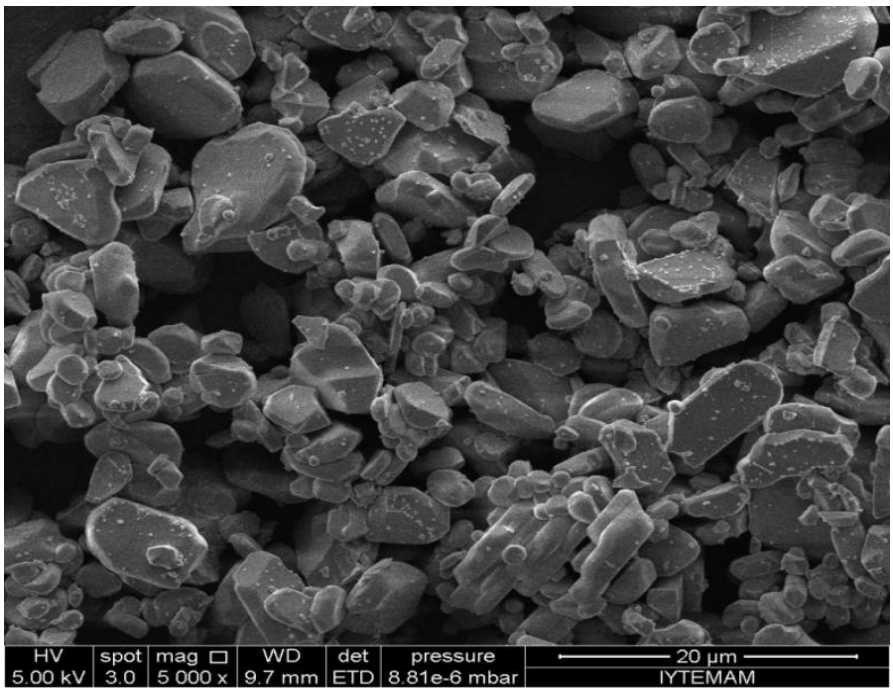

Figure 7.7. SEM image of CL 4400 FG 5.2 micron α-alumina powderat 5kX.

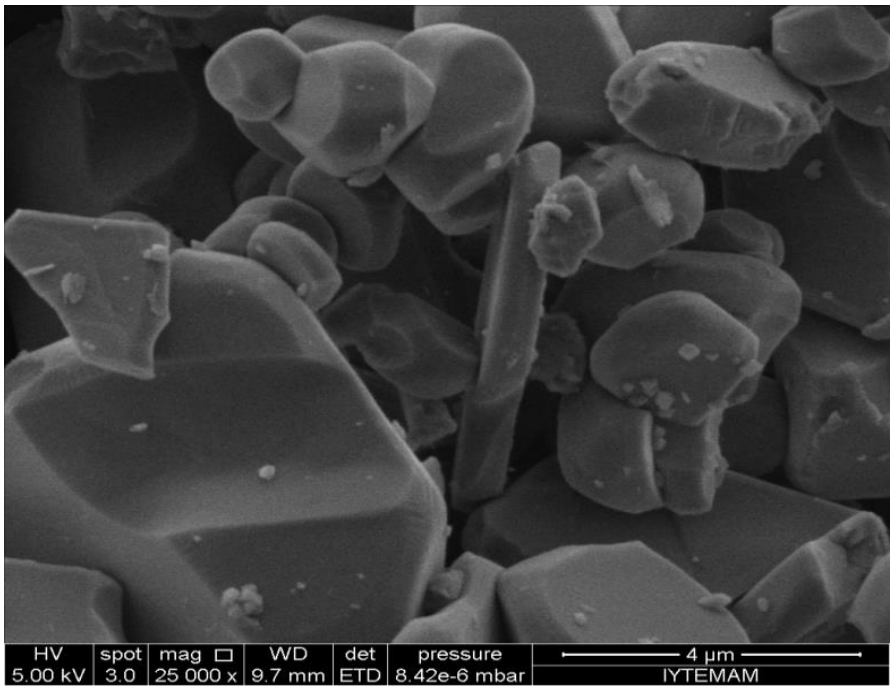

Figure 7.8. SEM image of the CL 4400 FG 5.2 micron α-alumina powder at 25kX.

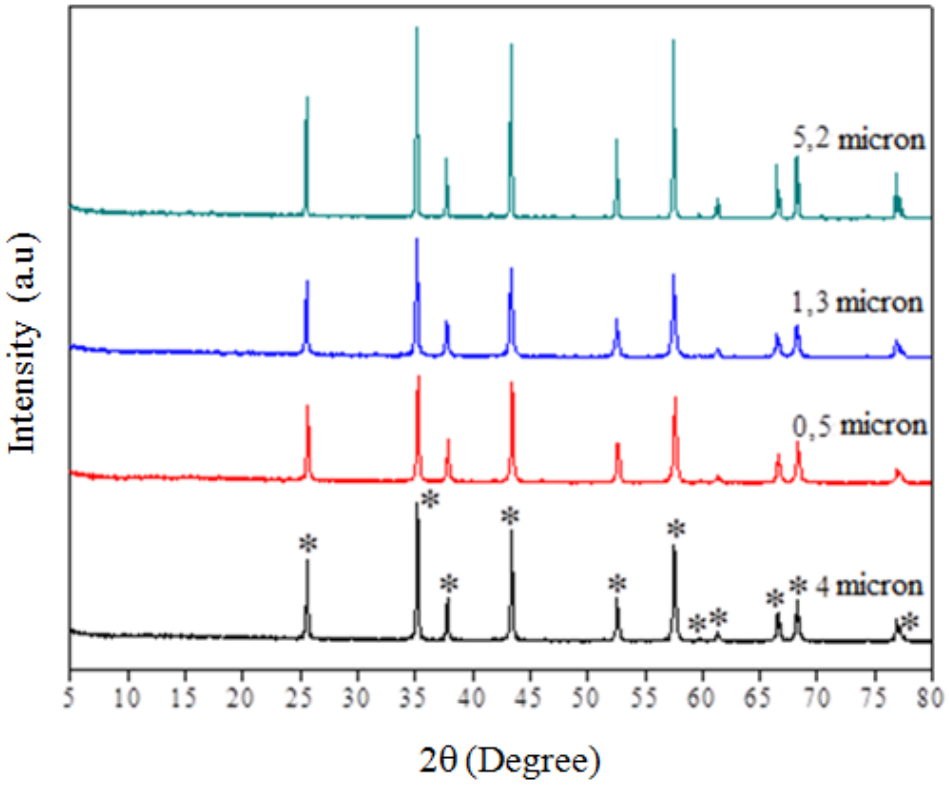

Figure 7.9. XRD patterns of α-Alumina powders (*α-alumina).

The properties of the boehmite powders as reported by the manufacturer are given in Tablo 7.2. UF1 layer was slip casted by using a stable boehmite sol. The SEM micrograph of the boehmite powder given in Figure 7.10 indicated that the crystallite size of the boehmite powder is in the nanoscale with platey primary particles. The XRD pattern of the powder given in Figure 7.11 indicated that they had boehmite phase structure with no impurity phases.

Table 7.2. The properties of boehmite (Sasol Co).

Particle Size/ d_{50} [nm]	25
BET Surface Area[m^2/g]	180
Dispersed Particle Size [nm]	80
Crystallite size [nm]	10

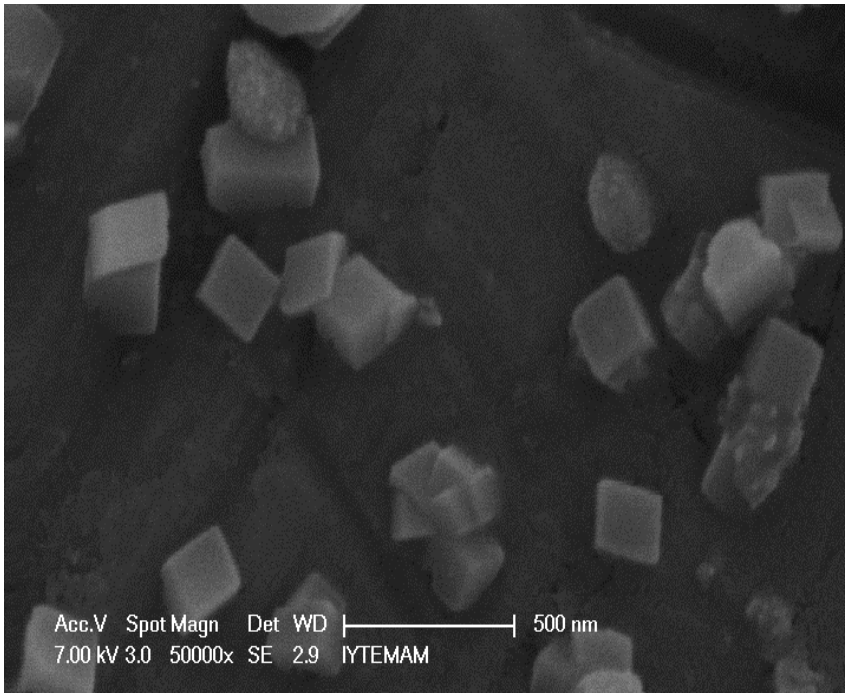

Figure 7.10. The SEM images of Boehmite (Disperal).

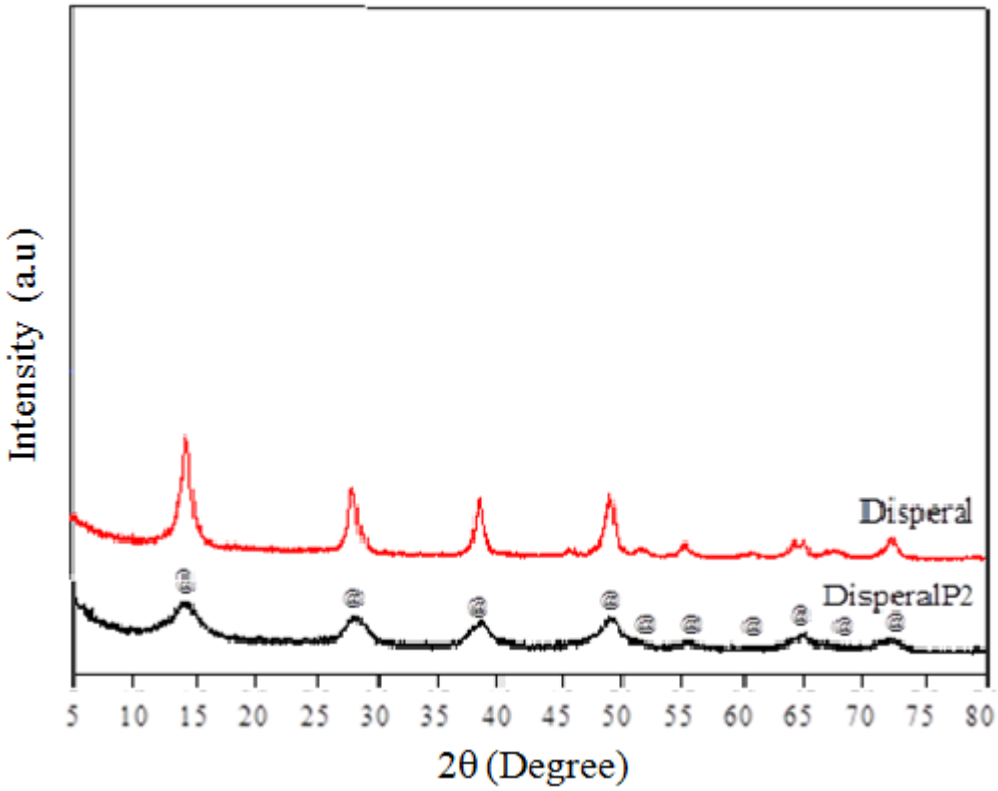

Figure 7.11. XRD patterns of boehmite.

7.2. Preparation of Selective Layers

The extruded heat treated tubular α-alumina supports are shown in Figure 7.12. The alumina supports were coated with two intermediate layers and a thin top layer with nanometer sized pores for the formation of an asymmetric membrane structure. The tubular alumina supports were slip casted with α-alumina suspension (MF), boehmite sol (UF1), titania hydrosol (UF2) and titania polymeric sol (NF) for the fabrication of the final membrane successively.

Figure 7.12. Extruded heat treated tubular alumina supports.

7.2.1 Selective Layer Sol Particle Size Analysis

Selective microfiltration and ultrafiltration layers were prepared by using α-alumina and boehmite colloidal suspensions. The particle size distribution of the α-alumina suspension is given in Figure 7.13 where the determined volume based average particle size was 522 nm.

The particle size distribution of the boehmite sol used for UF1 layer consolidation is given in Figure7.14 where the volume based average particle size was determined as 42 nm.

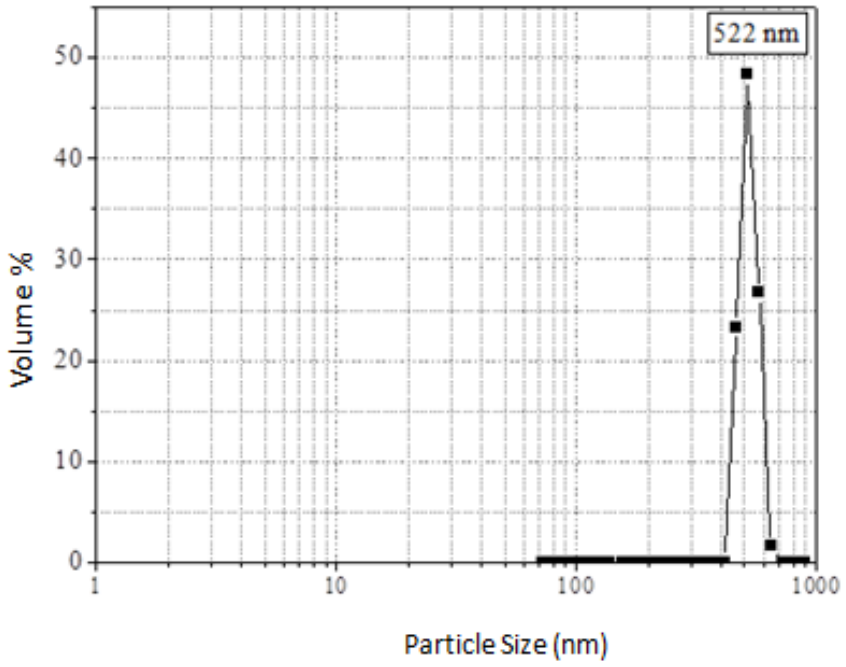

Figure 7.13. The volume based particle size distribution of 0,5µm α-alumina and 1% PVA suspension.

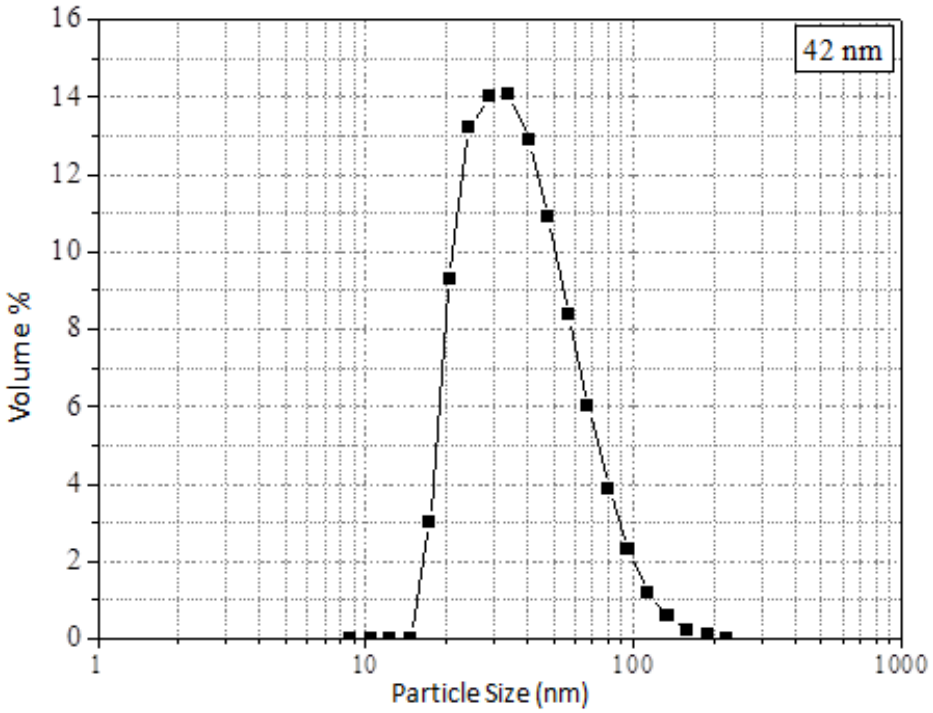

Figure 7.14. The volume based particle size distribution of 2wt% boehmite and 0.66 wt% PVA sol.

UF2 layer was prepared by using a TiO_2 hydrosol. The particle size of the titania sol was found to vary with the molar ratios of the titanium IV isopropoxide:

diethanolamine: nitric acid: water: propanol (TTIP:DEA:HNO_3:H_2O:Propanol) used in the hdrosol synthesis. The particle size distribution of the titania hydrosol (1:0.8:2.4:1000:10 molar ratio) is given in Figure 7.15 and the volume based particle size was determined as 14 nm. The volume based particle size distribution of another titania hydrosol (1:1.2:2.4:1000:20 molar ratio) with higher DEA and water contents is given in Figure 7.16 where the particle size was found as 18 nm indicating the possibility of the nanodesign of the selective layer pore structure through hydrosol particle size. The hydrosol particle size distribution presented in Fig 7.17 for another composition proved that the synthesis of 7 nm particles through the control of sol chemistry is possible.

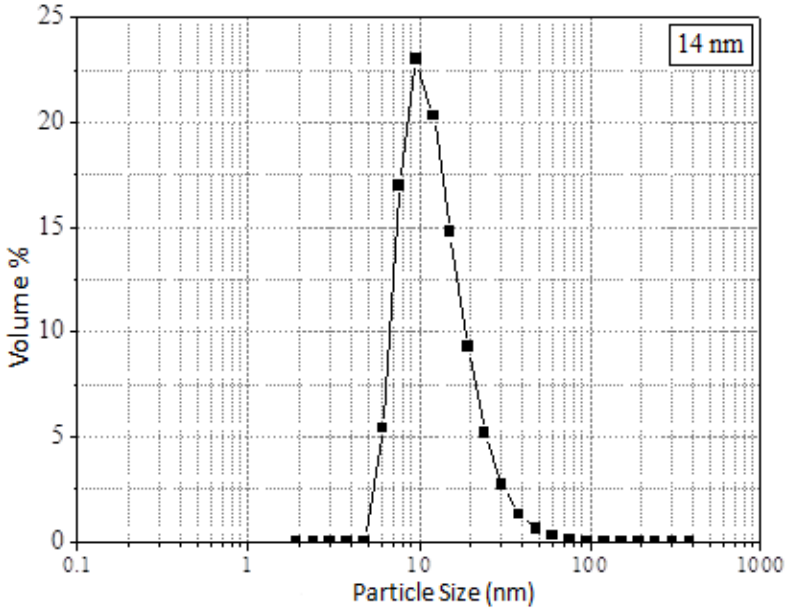

Figure 7.15. The volume based particle size distribution of the TiO_2 hydrosol (TTIP:DEA:HNO_3:H_2O: Propanol molar ratios set as 1:0.8:2.4:1000:10).

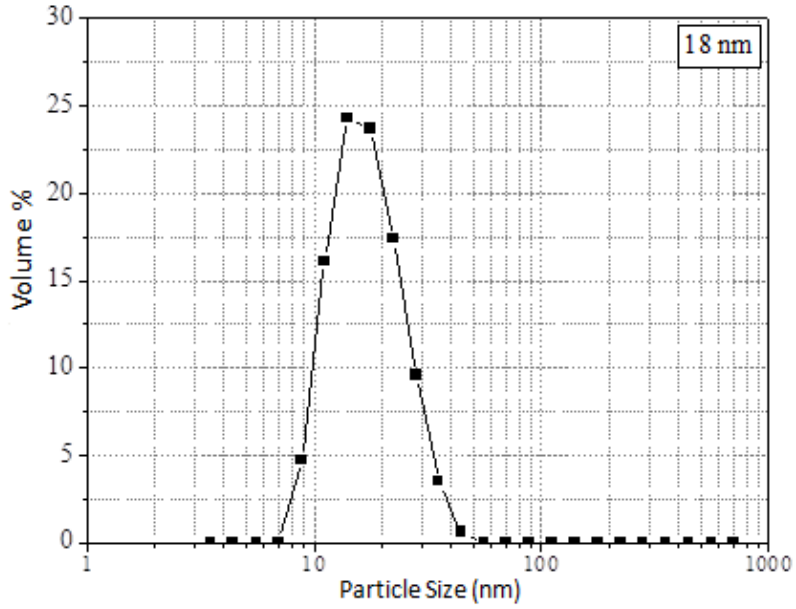

Figure 7.16. The volume based particle size distribution of TiO_2 hydrosol (TTIP:DEA:HNO_3:H_2O: Propanol molar ratio set as 1:1.2:2.4:1000:20).

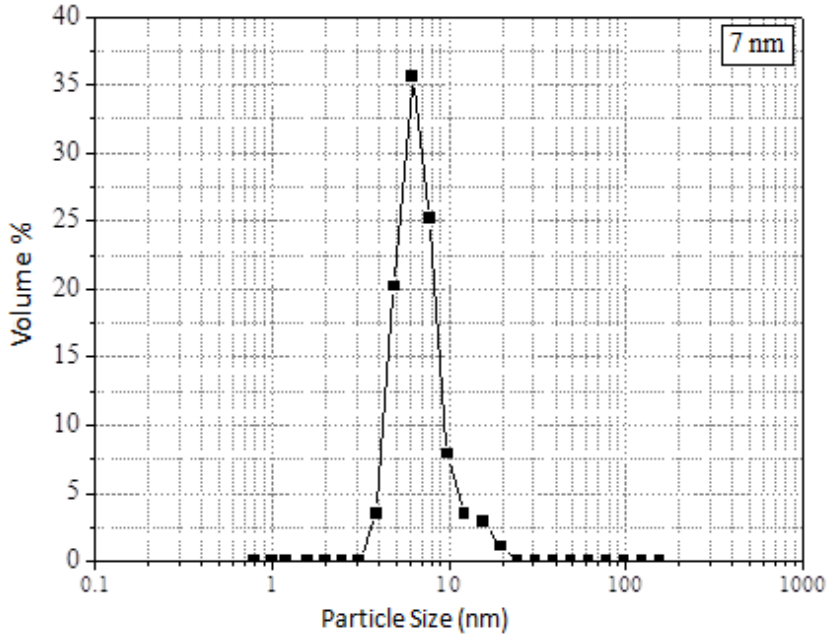

Figure 7.17. The volume based particle size distribution of TiO_2 hydrosol (TTIP:DEA:HNO_3:H_2O: Propanol molar ratio set as 1:0.8:2.4:500:20).

NF layer was prepared by using a polymeric titania sol. The particle size distribution of the polymeric titania sols prepared at a preset compositions are given in Figures 7.18 and 7.19 (TTIP:DEA:HNO_3:H_2O:Propanol molar ratios 1:1.2:0,057:2:52 and 1:1:0,057:2:52). The average particle sizes of the polymeric titania sols were found as 8 and 1 nm respectively.

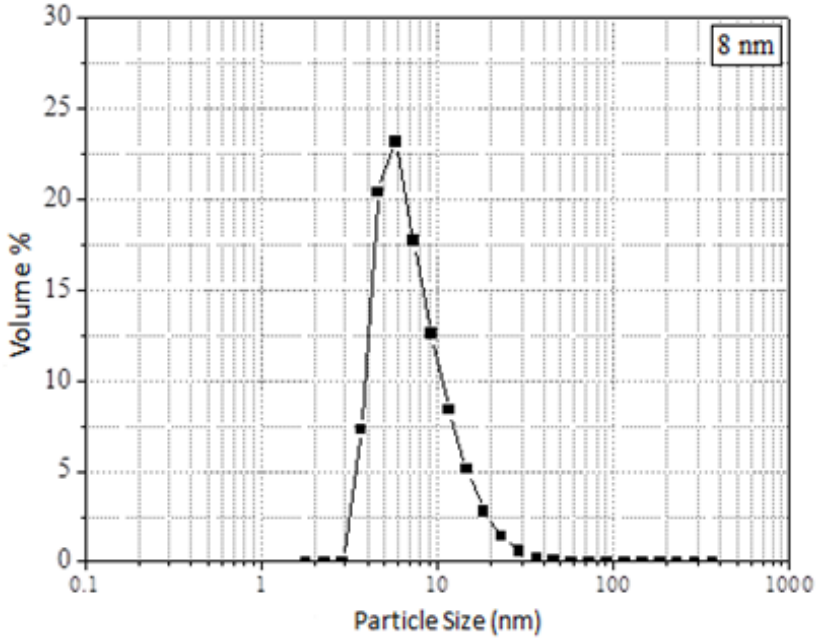

Figure 7.18. The particle size distribution of the polymeric TiO_2 sol (TTIP:DEA:HNO_3:H_2O:ETOH molar ratio 1:1.2:0,057:2:52).

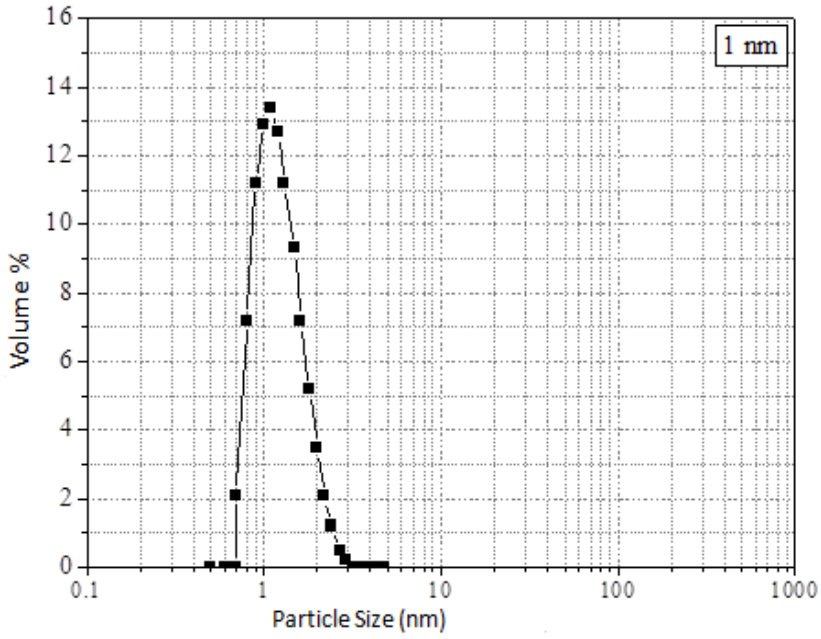

Figure 7.19. The particle size distribution of polymeric TiO_2 sol (TTIP:DEA:HNO_3:H_2O:ETOH molar ratio 1:1:0,057:2:52).

7.2.2 Heat Treatment of Selective Layers

The selective layers prepared through colloidal sol-gel based room temperature methods must be heat treated in order to thermally stabilize the thin layers with also increasing its mechanical/chemical durability. The heat treatment schedule/peak soak

temperature selection depends on the nanostructure of the selective layer and the organic/inorganic content of the sol along with the packing characteristics of the particles/species forming the sol. The determination of the shrinkage/densification behaviour of the unsopported films by high temperature dilatometry was used for the determination of these heat treatment schedules specific to the nature of the selective layer. The variation of the green compact shrinkage frequency and percentage (heating rate:4 ^{o}C/min) as a function of temperature of the room temperature dried 0.5μm α-alumina MF layer unsupported powder was determined by dilatometry runs and are given in Figures 7.20 and 7.21. The dilatometric curve of 0.5 micron alumina pellet indicates a large shrinkage and a fast densification between 1000 ^{o}C to 1200 ^{o}C (Corresponding to the peak labelled as 2 in Figure 7.20). A relatively slow heat treatment was chosen for the heat treatment of the selective MF layers in line with the above information in order to prevent the formation of cracks in the MF film bulk/surface. The heating rate was decreased from 4^{o}C to 2^{o}C/min in order to prepare defect free MF layers with smooth surfaces. The conditions applied for the heat treatment of the 0.5μm α-alumina coated membranes were selected based on this dilatometric investigation which was previously stated in Chapter 6.3 in the experimental section.

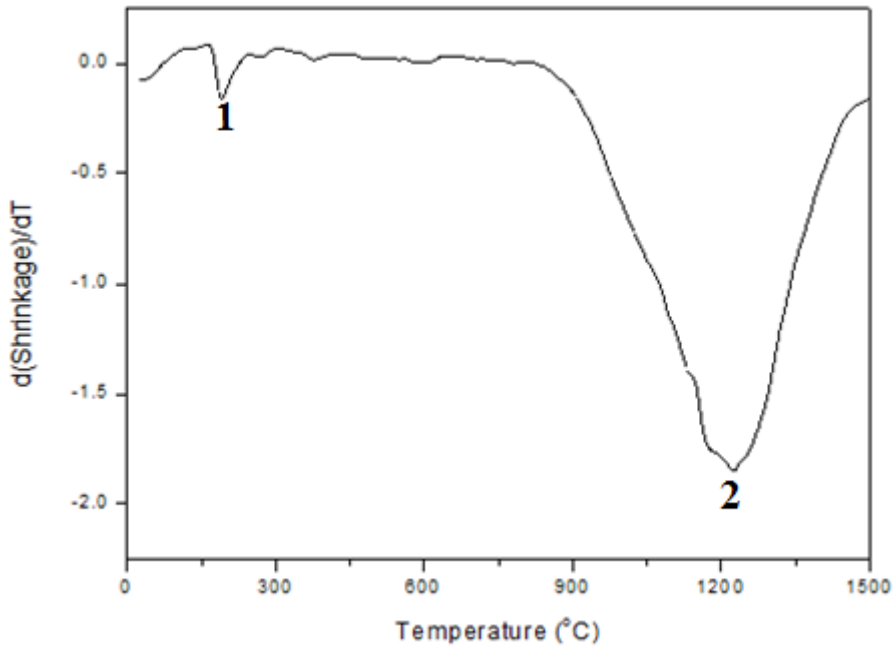

Figure 7.20. The dilatometric frequency curve of dried unsupported 0.5 micron alumina MF membrane selective layer.

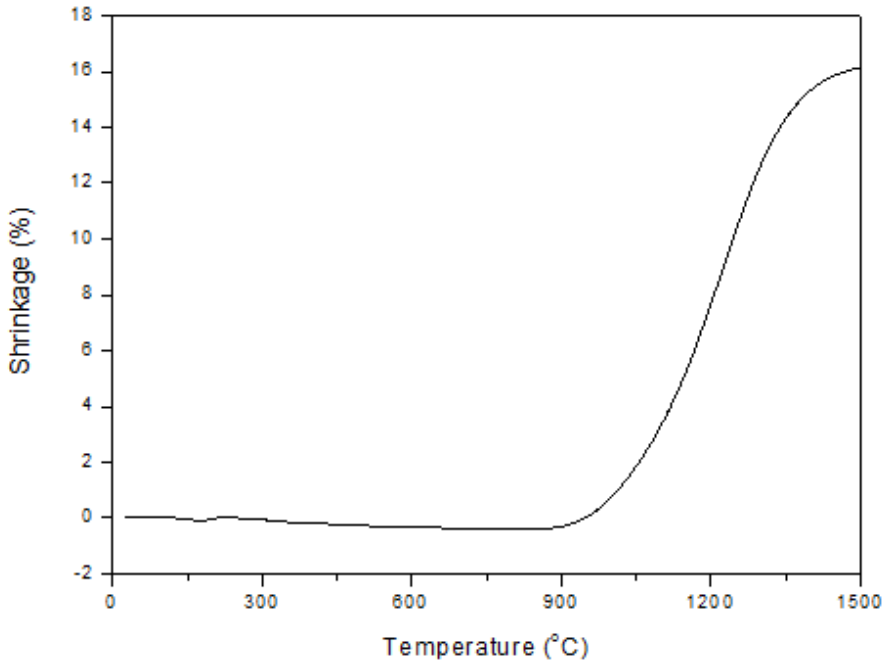

Figure 7.21. The dilatometric percentage shrinkage curve of dried unsupported 0.5 micron alumina MF membrane layer.

The dilatometric curve of dried unsupported boehmite membrane is shown in Figures 7.22 and Figure 7.23. Large shrinkages were observed in the 100-150^{o}C and 200-400^{o}C ranges. The changes in the pellet dimensions in between 400^{o}C to 600 ^{o}C was very low indicating a relatively stable film nanostructure in this range where also the heat treatment conditions may be less effective on surface/bulk defect generation. The first peak (1 in Figure 7.22) most likely is due to the densification as a result of physical/chemically bound water loss whereas the second peak is related with boehmite decomposition/phase transformation to a transition alumina (which may yield γ-alumina at 600^{o}C). The final peak (peak labelled as 3) in the same figure is most likely related with the γ-Al_2O_3 to α-Al_2O_3 phase transformation.

The heating rate was decreased from 4^{o}C to 1^{o}C/min in order to minimize the defect/crack formation in the UF1 film in the 200-400^{o}C range where shrinkage rate was determined to be significantly high. The boehmite coated membrane was further heat treated and soaked at 600 ^{o}C as was explained in Chapter 6.3 in accordance with this dilatometric behaviour.

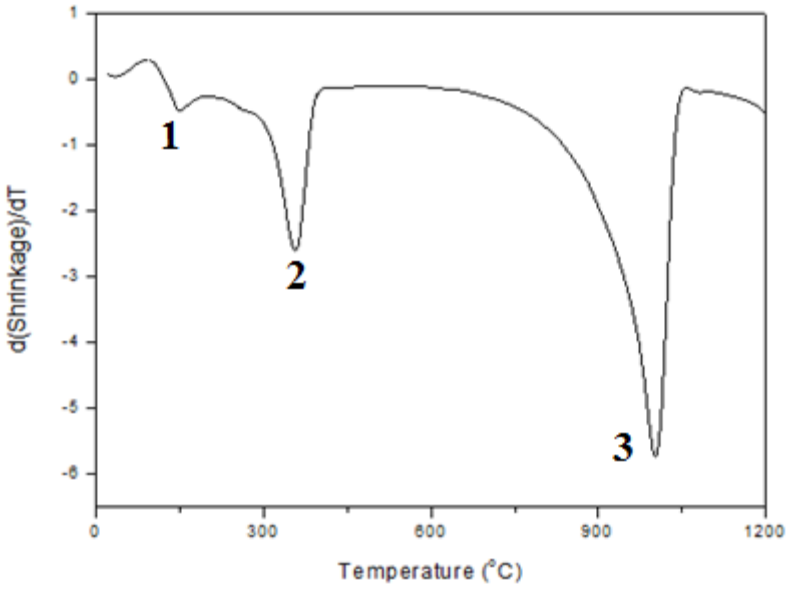

Figure 7.22. The dilatometric frequency curve of dried unsupported UF1 boehmite. membrane selective layer.

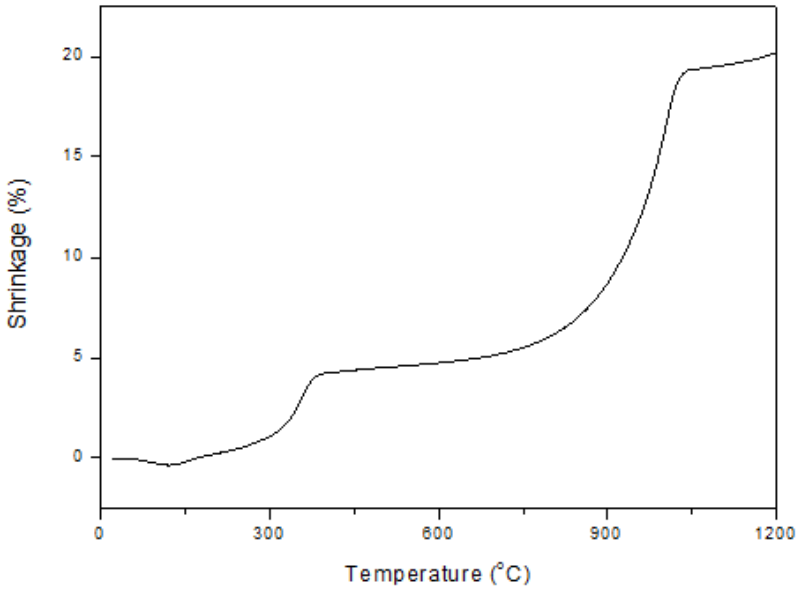

Figure 7.23. The dilatometric percentage shrinkage curve of dried supported UF1 boehmite selective membrane layer.

The dilatometric frequency/shrinkage percentage vs temperature behaviour of unsupported titania membrane pellet is shown in Figures 7.24 and 7.25. The first dilatometric peak was located at about 100^{o}C which was due to ethanol/water removal related pking in the structure. The titania pellet dimension decreased by about %5 as a result of this phenomena. The second peak was located in between 200-300^{o}C which was related with amorphous-crystalline TiO_2 phase transformation. The main

dilatometric peak was located in the relatively broad 375-550^{o}C range. The anatase crystallite particle growth/densification along with partial anatase to rutile phase transformation is likely to occur in this temperature range where thin nanofiltration top layers are commonly heat treated. The shrinkage gradually continued up to about 600^{o}C with three faster shrinking regions. The determination of the heat treatment was obviously not very easy for crack-free nanofiltration layer formation. A relatively low heating rate was set at 1^{o}C/min in accordance with this finding for heating up to 400^{o}C with 60 minutes soak at this peak temperature as was stated in Chapter 6.3 of the experimental section.

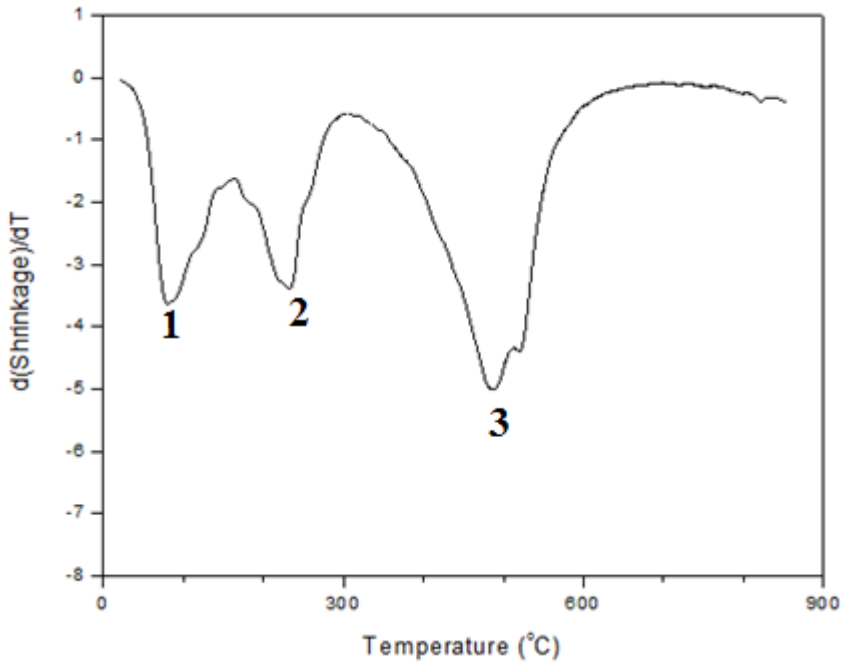

Figure 7.24. The dilatometric frequency curve of unsupported titania NF membrane top layer.

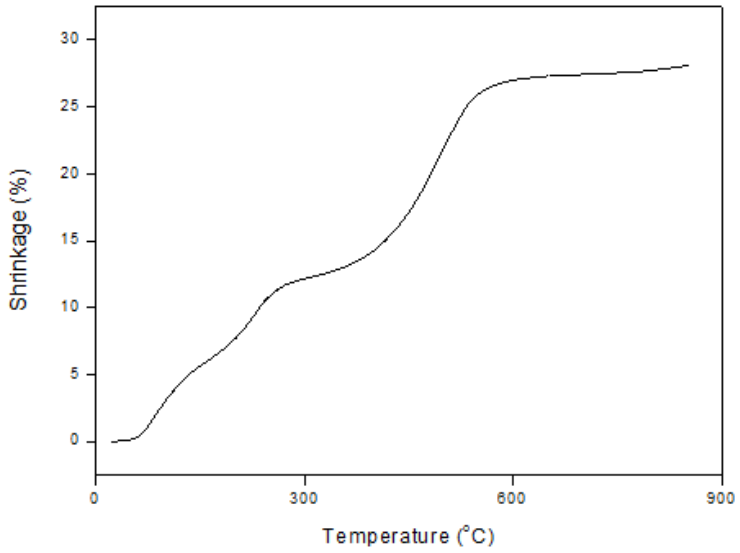

Figure 7.25. The dilatometric percentage shrinkage curve of unsupported titania NF membrane top layer.

7.2.3 Optical Microscope Investigation

The effect of heating rate on membrane surface layer was investigated by optical microscopy(OM) at two levels. The OM image of 0.5μm α-alumina coated MF membrane surface heat treated with 4°C/min rate is given in Figure 7.26. Although cracks were formed on the surface of the MF layer at this high rate, the surface became smooth and crack-free when the rate was lowered to 2°C/min as shown in Figure 7.27.

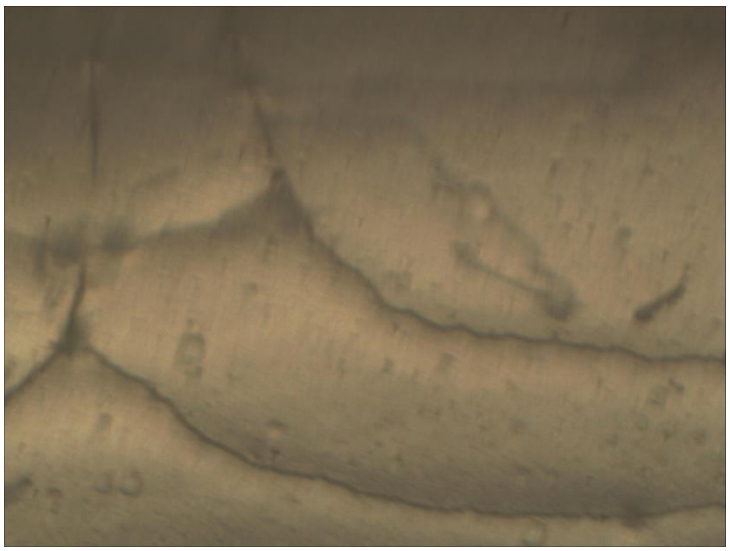

Figure 7.26. Optical microscope image of 0.5 μm α-alumina coated membrane MF surface heated with 4°C/min rate to the peak 1200°C soak temperature.

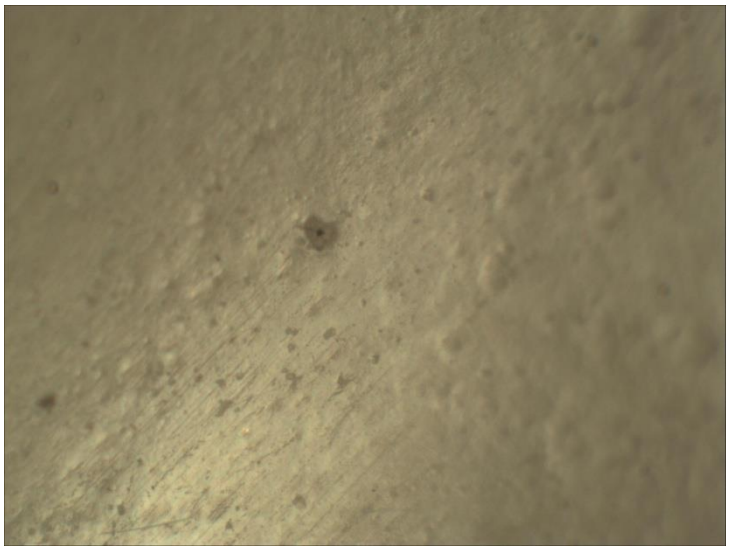

Figure 7.27. Optical microscope image of 0.5 μm α-alumina coated membrane MF surface heated with 2°C/min rate to the peak 1200°C soak temperature.

Optical microscope image of boehmite (UF1) coated membrane surface with 4°C/min heat treatment rate is given in Figure 7.28. The membrane surface was cracked seriously and in order to slow down shrinkage and prevent crack formation in the 200°C to 400 °C range the heating rate was decreased from 4°C to 1°C/min. The boehmite coated UF1 layer surface became continuous and crack-free after heat treatment with the lower heating rate as shown in Figure 7.29.

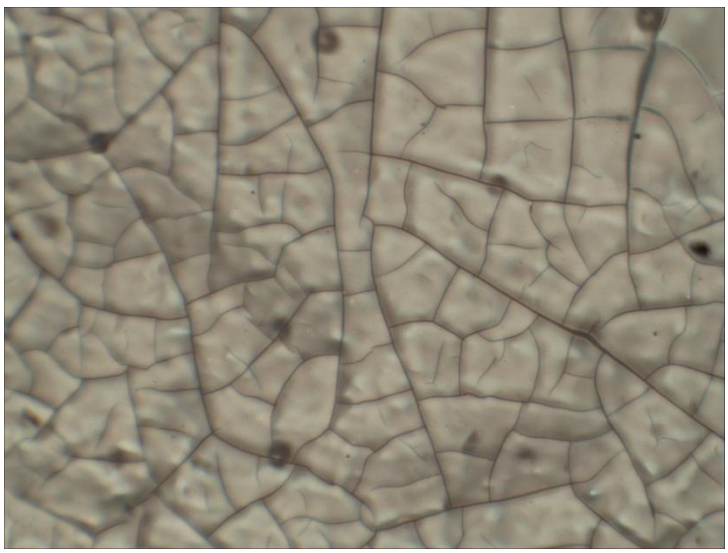

Figure 7.28. Optical microscope image of boehmite coated UF1 membrane surface heat treated with 4°C/min rate in the 200-400°C range.

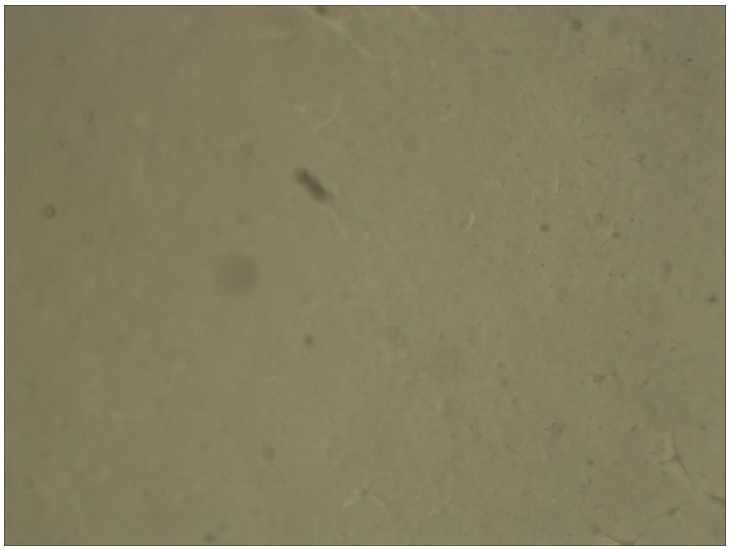

Figure 7.29. Optical microscope image of boehmite coated UF1 membrane surface heat treated with 1^{o}C/min rate in the 200-400^{o}C range.

The optical microscope image of titania (UF2) coated membrane surface with a heat treatment rate of 4^{o}C/min is shown in Figure 7.30. There were many cracks on the surface due most likely to the relatively fast shrinkage rate whereas the same titania (UF2) coated surface when heat treated with 1^{o}C/min heat treatment rate became more continuous and crack-free as seen in Figure 7.31.

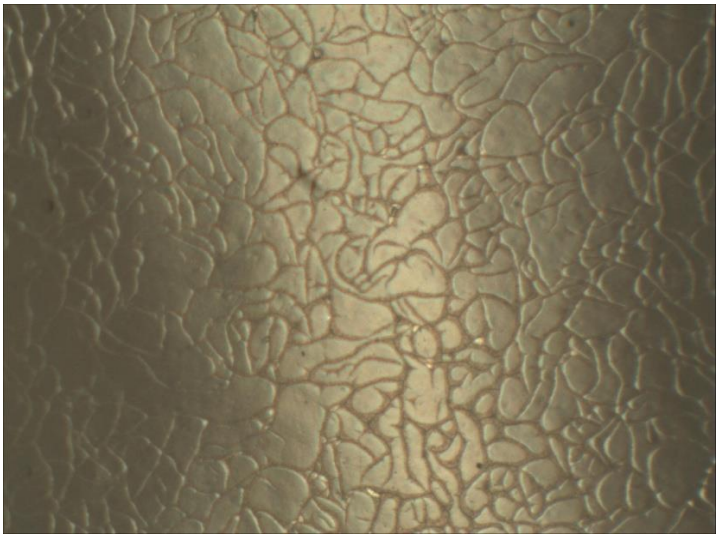

Figure 7.30. Optical microscope image of heat treated titania (UF2) coated membrane surface with a rate of 4^{o}C/min.

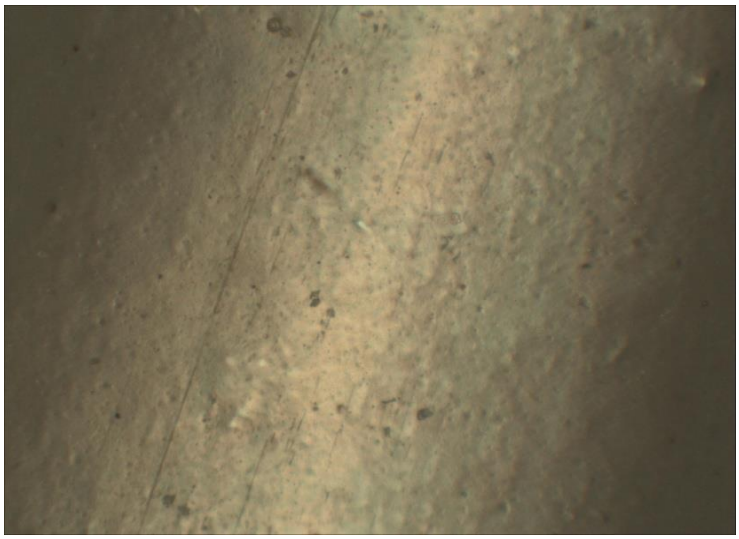

Figure 7.31. Optical microscope image of heat treated titania hydrosol coated UF2 membrane surface with a rate of 1^{o}C/min.

7.2.4 Scanning Electron Microscope Investigation

The tubular ceramic membrane was composed of three layers (two ultrafiltration layers and a microfiltration layer) on the α-alumina tubular support. The SEM images of the surfaces and the cross-sections of the microfiltration membrane layer on the support is shown in Figure 7.32. The images show that the membrane surface was morphologically homogenous, smooth and free of cracks. The PVA use as a drying controll additive was more effective in preventing crack formation. The average thickness of the microfiltration layer was approximately about 50 microns.

The ultrafiltration membrane consisted of a double-coated layer on the microfiltration layer. The UF1 layer surface was smooth and crack-free. Small cracks and damage on the UF1 layer may have been created during sample preparation for SEM where breaking/cutting of the tubes for inner surface investigation wa inevitable. It can be seen that there are no cracks on first/second ultrafiltration layers and also the adhesion level between the layers is quite satisfactory. The thickness of the UF1 layer was about 3 μm and the thickness of the UF2 layer is 733 nm as stated in Figure 7.34. Total thickness of the ultrafiltration layer was around 3.59 microns.

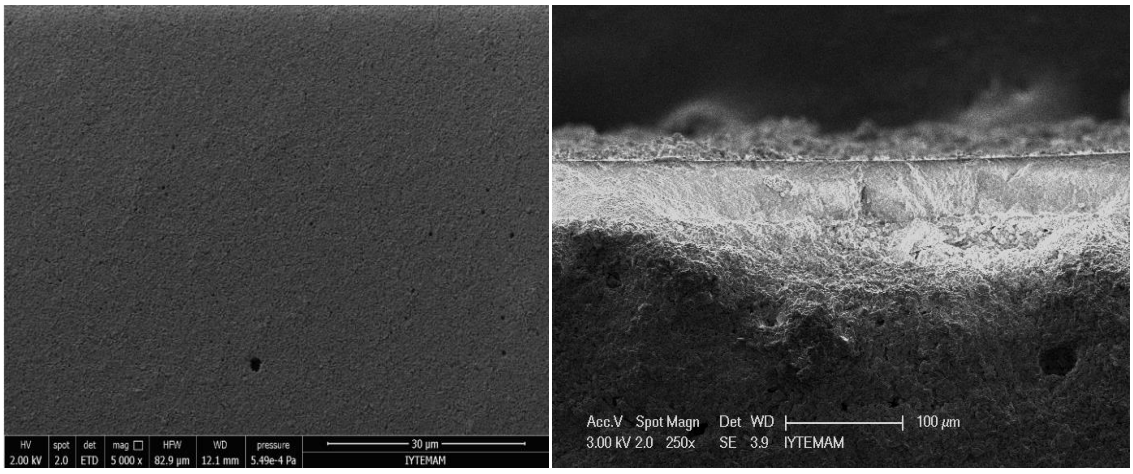

Figure 7.32. SEM images of the ceramic microfiltration membrane surface and its cross section.

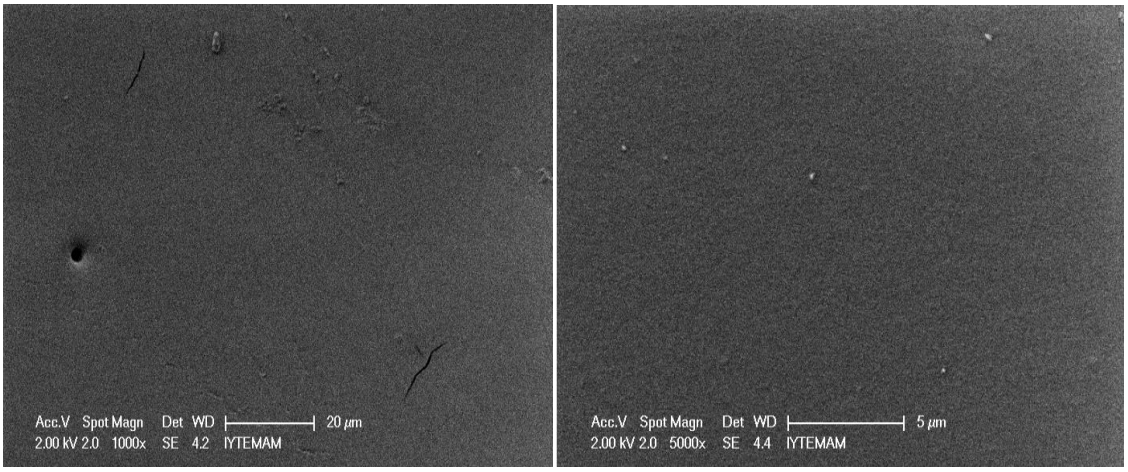

Figure 7.33. SEM images of the ceramic UF1 layer surfaces.

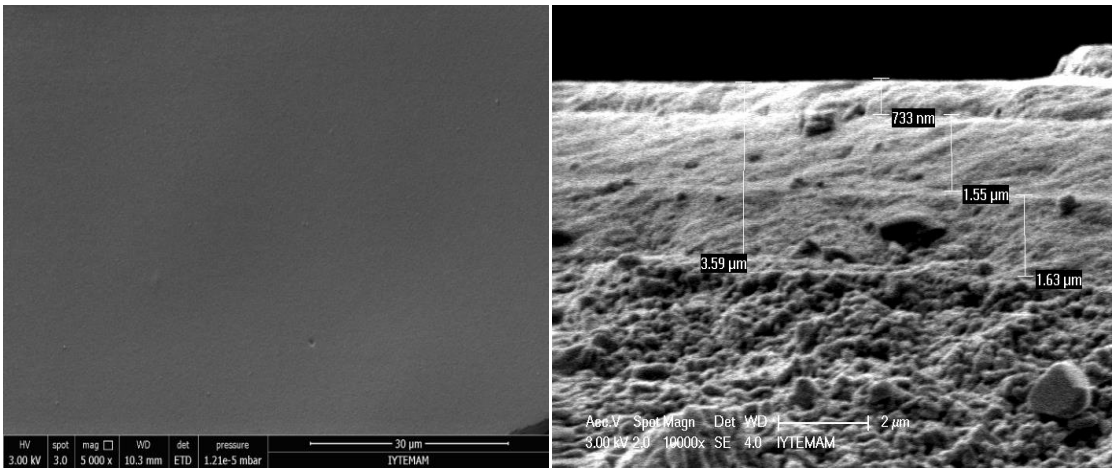

Figure 7.34. SEM images of the UF2 layer surface and its cross section showing selective layers thicknesses.

7.3 Membrane Performance

Characterization results of the received Sun Tekstil wastewaters is given in Table 7.3. The Pt-Co(465nm) values for the wastewaters before biological treatment were determined to be about 5100-5200 whereas this was decreased to about 3800 after biological treatment in the company site. The suspended solids content was quite high before biological treatment (~250 mg/L) which was significantly reduced with biological treatment to about 74 mg/L. The COD decreased from 350-360 mg/L to 187 mg/L with biological treatment. The TOC values varied in the 281-86 mg/L range.

Variation of the clean water flux with respect filtration pressure of all the prepared membranes and supports are given in Figure 7.35. The membrane flux increases with increasing pressure (TMP) as expected. The macroporous supports displayed the highest fluxes (as high as ~3000 L/m^2h) which was decreased to about 100 L/ m^2h after the UF2 layer was formed on the inner surface of the tubular membranes. Almost a linear relationship was present between the flux and the filtration pressure.

The flux decline behaviour of the membranes during the filtration of the three wastewaters are presented successively in Figures 7.36 through 7.38. The filtration pressure was set constant at 4 bar during these experiments. The flux of all the membranes was decreased significantly with time due to fouling. The fouling extent in the first filtration stage with the support tubes proved to the highest due to the presence of a high suspended solids content especially in the wastewaters received prior to biological treatment at the plant site. The fouling in the membranes with MF, UF1 and UF2 selective layers were lower compared to the bare support due to the successive nature of the conducted filtration experiments (The permeate from the support filtration fed as feed to the MF filtration, Mf permeate fed as feed to the UF filtration runs). The final stabilized fluxes of the MF-UF membranes was about 50 L/m^2h for the biologiclly treated wastewaters.

The suspended solids content of wastewater1 values were reduced 60% after the buncher funnel filtration pretreatment. After the support filtration pretreatment of wastewaters 2 and 3, the suspended solids contents were reduced about 92-93%. The funnel and support pretreatment significantly increased the performances of the membranes with MF, UF1 and UF2 selective layers.

The cumulative percent rejection values of all wastewaters after UF2 treatment are given in Table 7.4. For wastewater-1 permeate, cumulative percent color , suspended solids, conductivity, COD and TOC rejections were obtained as 90-93%, 99%, 29%, 60%, 79% respectively. For wastewater-2 permeate, cumulative percent color , suspended solid, conductivity, COD and TOC rejections were obtained as 78-87%, 97%, 16.3%, 53%, 66.5% respectively. The cumulative percent color, suspended solids, conductivity, COD and TOC rejections were obtained as 84-88%, 92.6%, 28.5%, 58%, and 75.7% for wastewater-3 permeate, respectively. These findings are also presented in the form of bar graphs in Figures 7.39 to 7.47.

Table 7.3. Characterization of textile wastewaters.

Parameter	**Wastewater**		
	1	**2**	**3**
Pt-Co (410 nm)	1532	1053	1378
Pt-Co (455 nm)	5140	3814	5150
Pt-Co (465 nm)	5198	3811	5210
Color (m^{-1})			
436 nm	73.2	54.4	72.2
525 nm	54.8	40.2	52.4
620 nm	34.2	22.6	25.6
Suspended Solid (mg/L) (810nm)	254	74	252
Conductivity (mS/cm)	12	13.35	18.54
Ph	7.5	8.31	10.22
COD (mg/L) (448 nm)	360	187.2	349
TOC(mg/L)	281.3	54.13	85.8

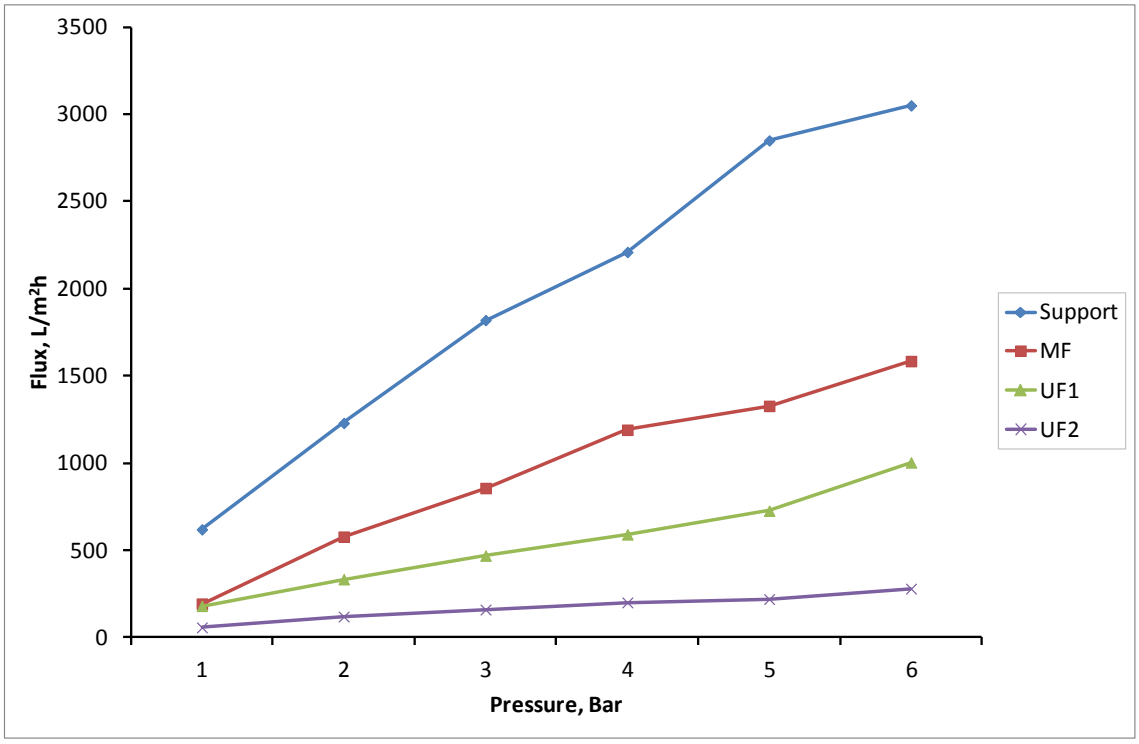

Figure 7.35. Variation of clean water flux with respect to pressure.

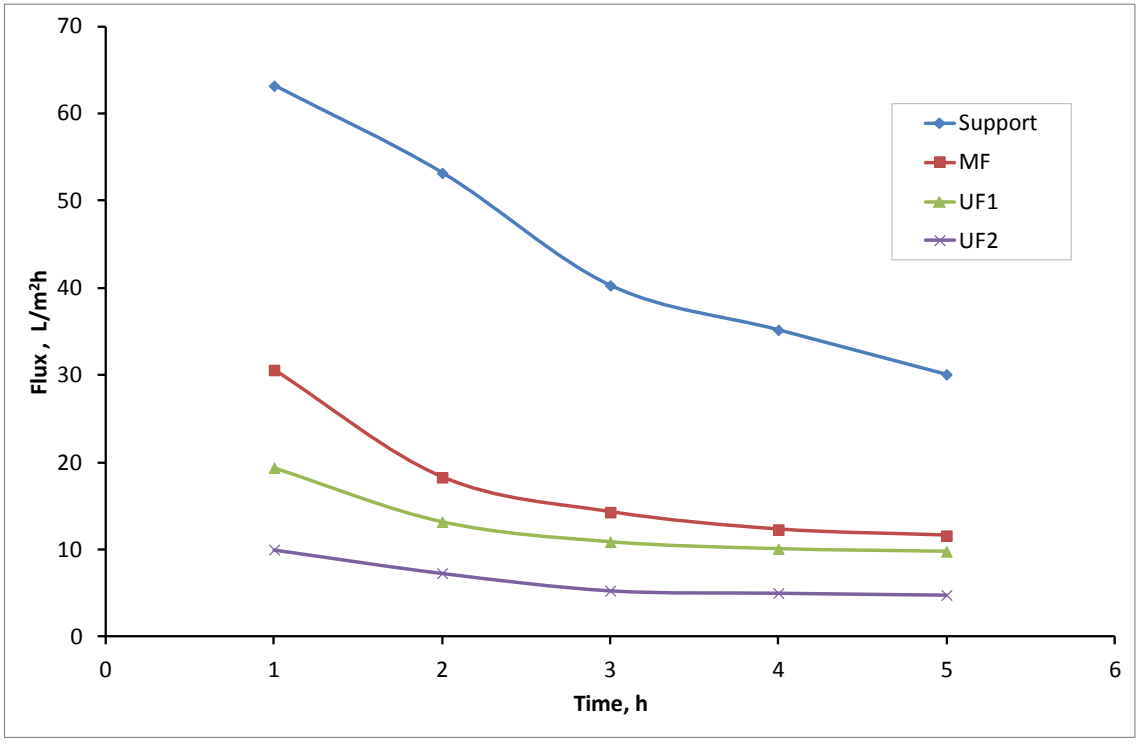

Figure 7.36. Flux decline of membranes at 4 bar (wastewater1).

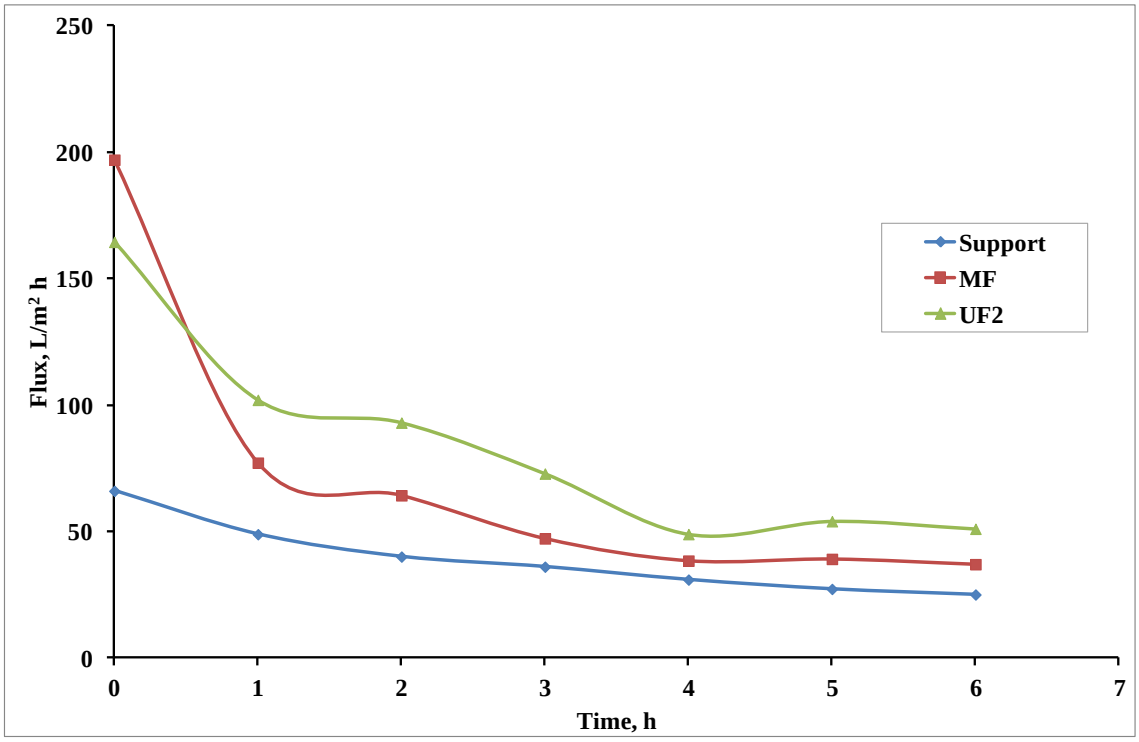

Figure 7.37. Flux decline of membranes at 4 bar (wastewater2).

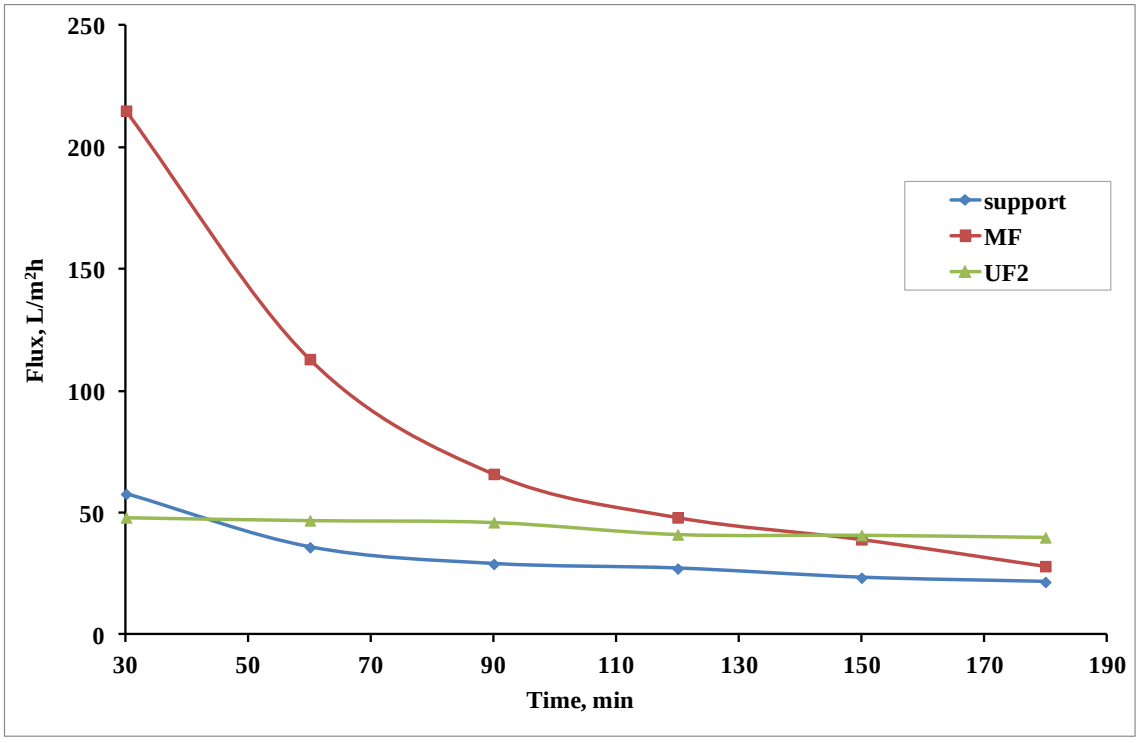

Figure 7.38. Flux decline of membranes at 4 bar (wastewater3).

Table 7.4. The cumulative percent rejection values of the wastewaters after the UF2 treatment.

Parameter	Waste Water		
	1	2	3
Pt-Co (410 nm)	90.60	78.50	86.20
Pt-Co (455 nm)	89.94	82.00	85.40
Pt-Co (465 nm)	90.04	81.00	85.70
Color (m^{-1}) 436 nm 525 nm 620 nm	 91.50 88.81 93.33	 81.20 80.40 87.53	 86.00 84.65 88.00
Suspended solid (mg/L) (810 nm)	98.81	97.46	92.60
Conductivity(mS/cm)	29.42	16.33	28.53
COD(mg/L) (448 nm)	60.00	53.00	58.00
TOC(mg/L)	79.04	66.56	75.75

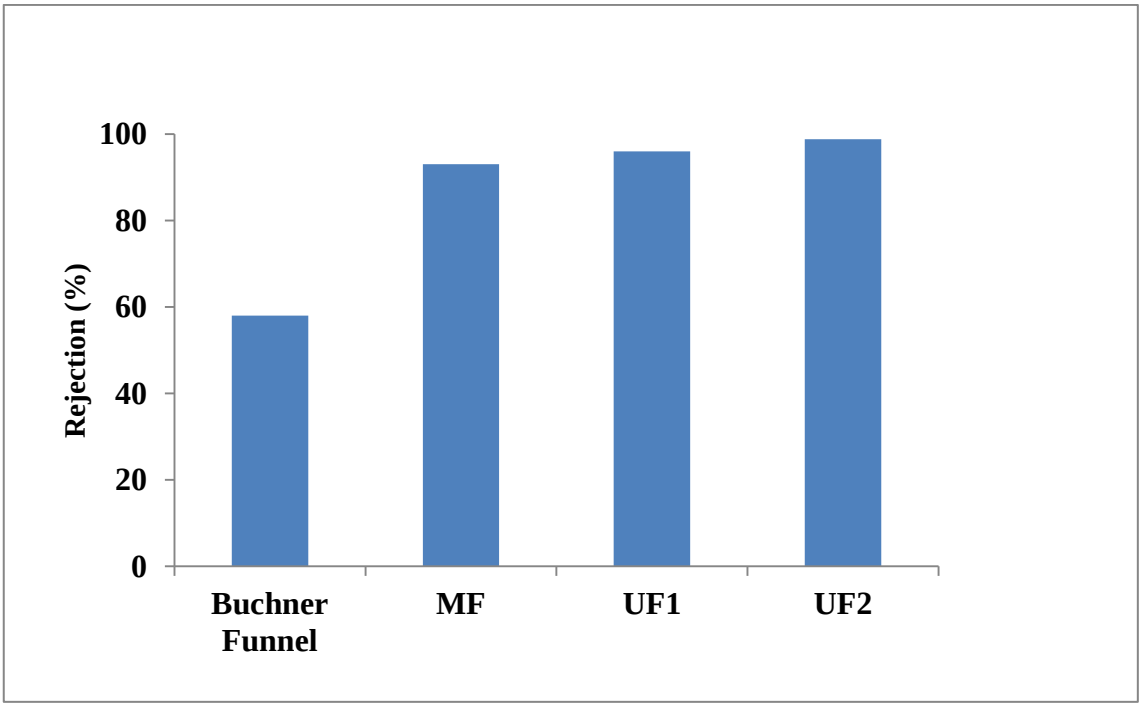

Figure 7.39. Rejection percentage of suspended solid (wastewater-1).

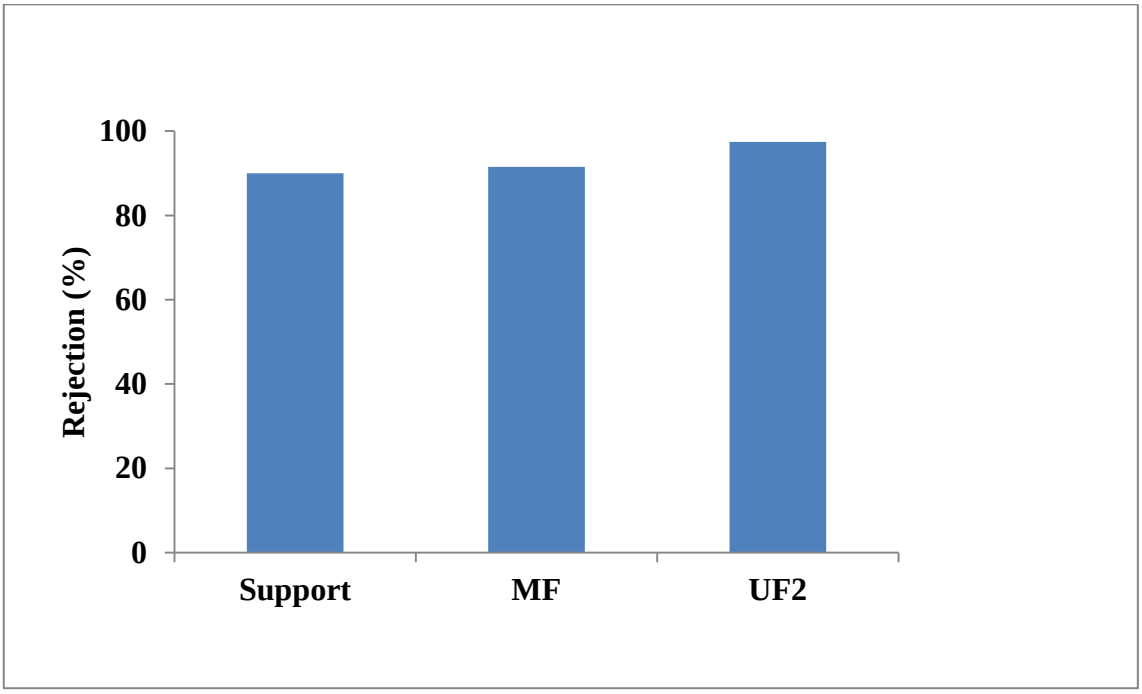

Figure 7.40. Rejection percentage of suspended solids (wastewater-2).

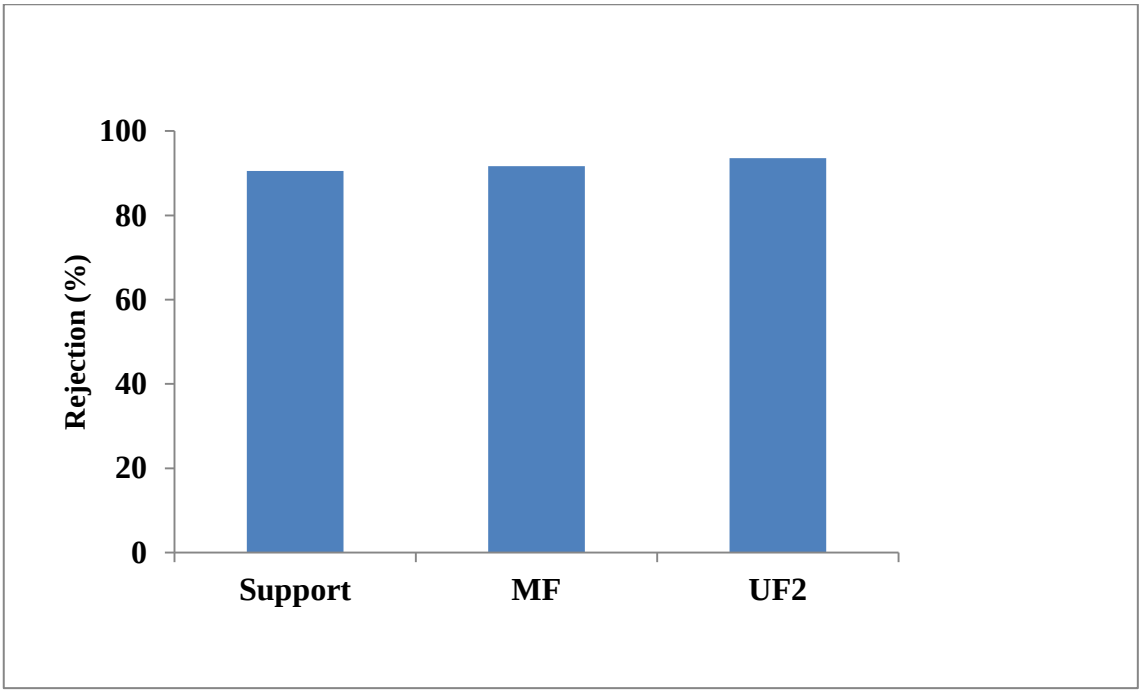

Figure 7.41. Rejection percentage of suspended solids (wastewater-3).

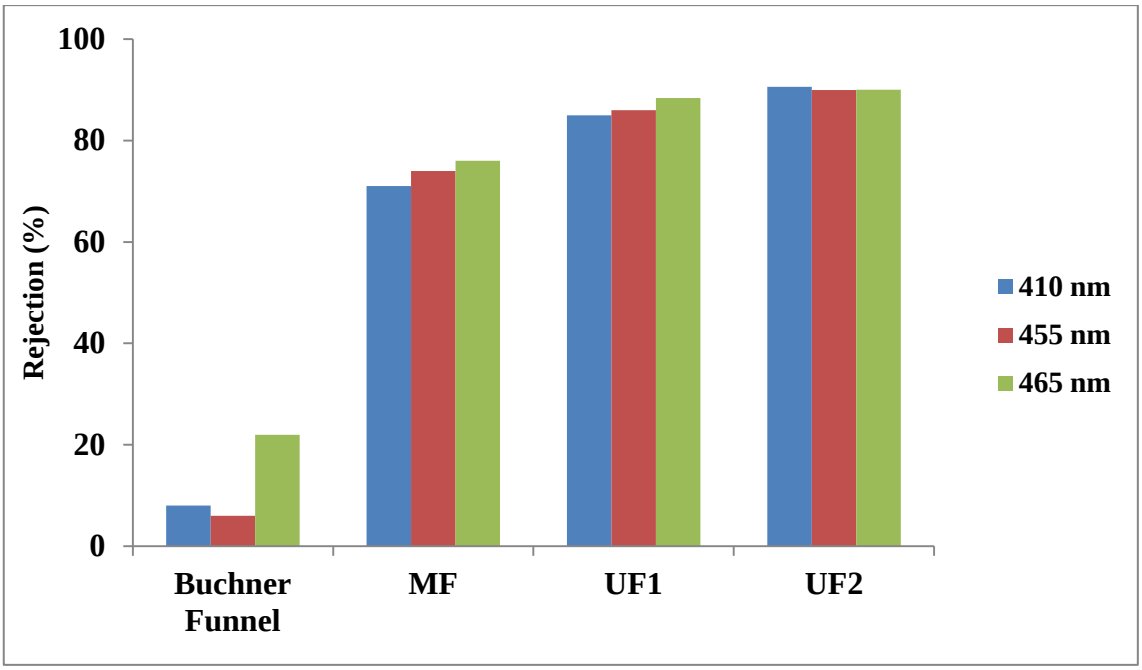

Figure 7.42. Rejection percentage of Color (Pt-Co) wastewater1.

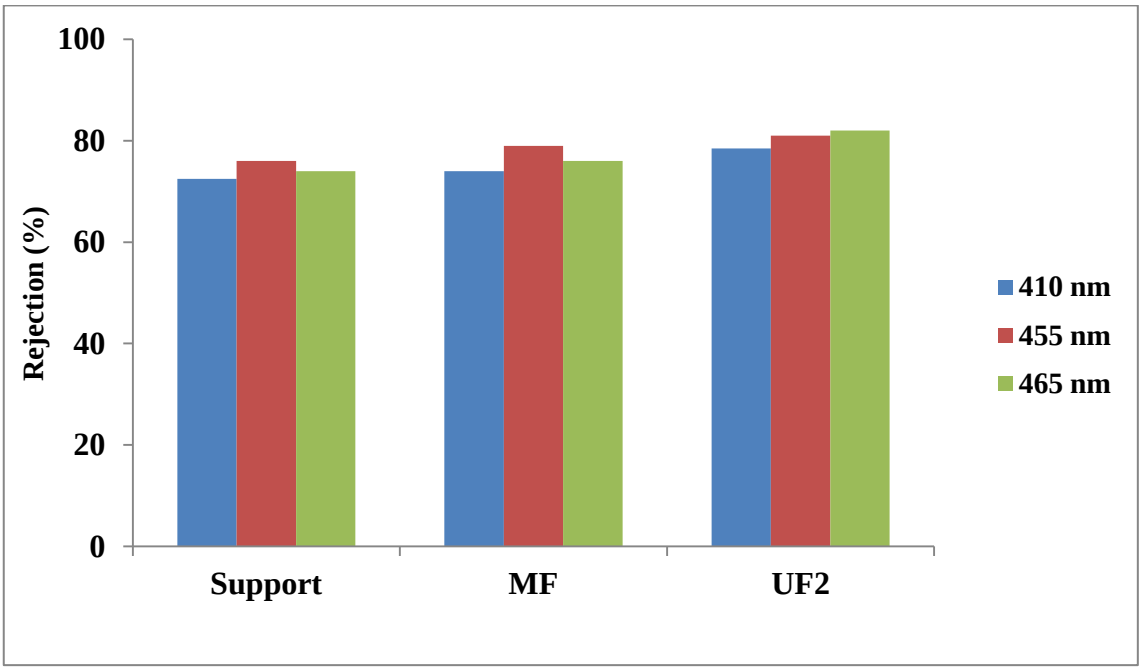

Figure 7.43. Rejection percentage of Color (Pt-Co) wastewater-2.

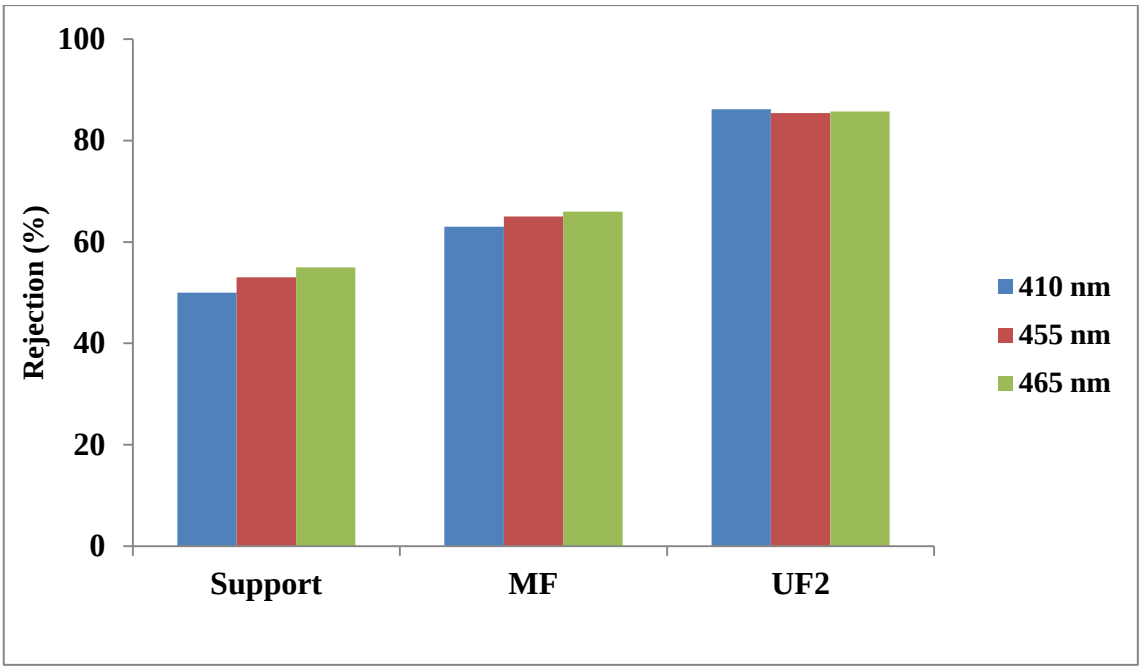

Figure 7.44. Rejection percentage of Color (Pt-Co) wastewater-3.

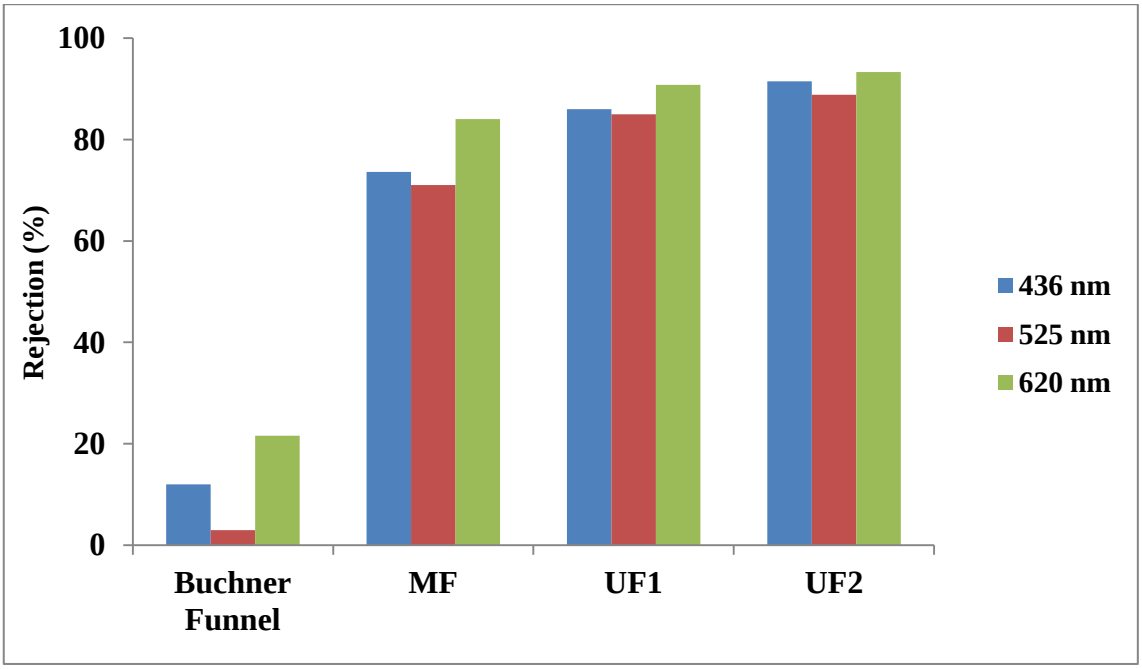

Figure 7.45. Rejection percentage of Color (m^{-1}) wastewater-1.

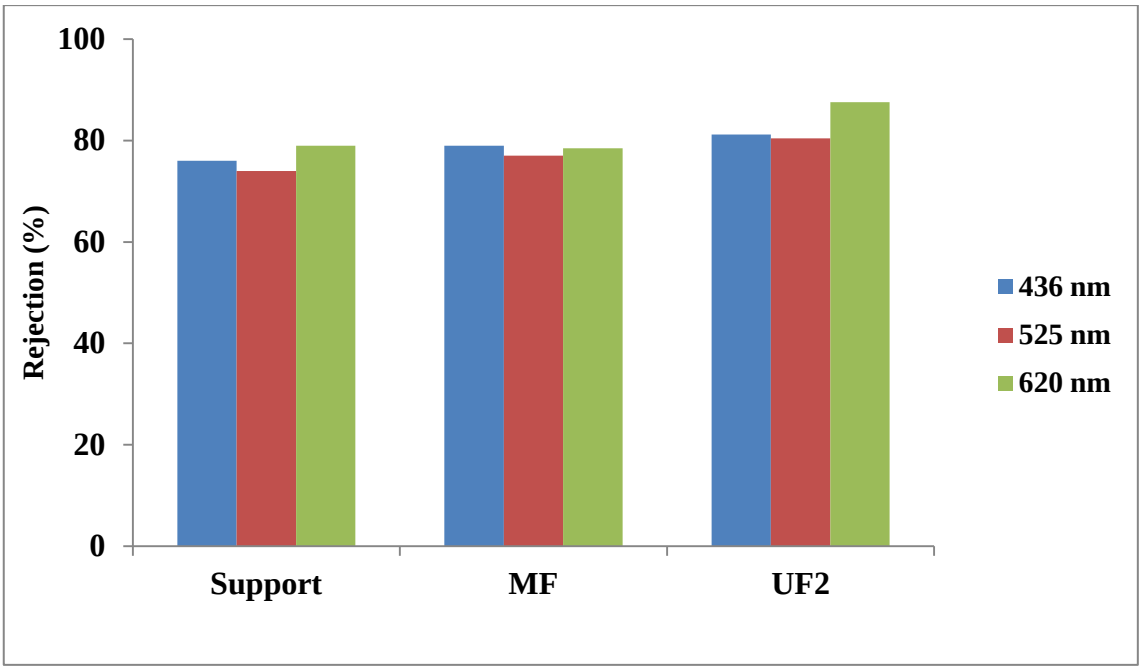

Figure 7.46. Rejection percentage of Color (m^{-1}) wastewater-2.

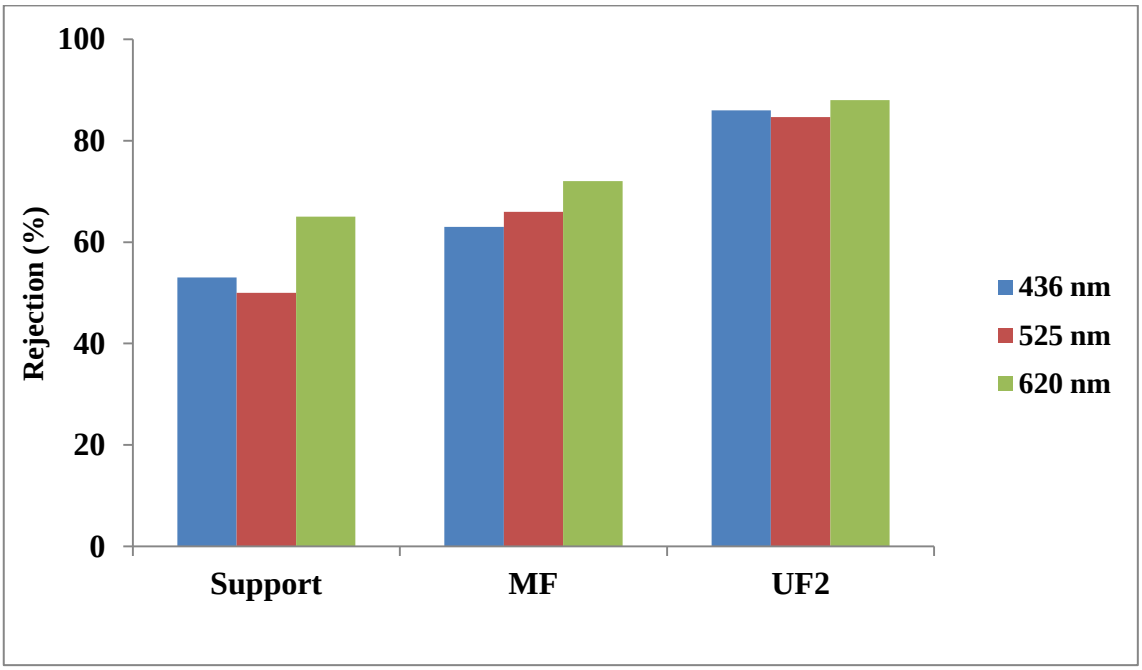

Figure 7.47. Rejection percentage of Color (m^{-1}) wastewater-3.

7.4 Membrane Fouling Analysis

The decline in the flux during the filtration runs with uncoated tubular support, MF and UF1 selective layer coated membranes were determined and tabulated in Table 7.5. The tubular uncoated support membrane had the highest flux decline due to the formation of a thick cake on the surface since most of the present suspended solids in the received wastewater were rejected during this first stage of membrane treatment. The flux decline was significantly lower for the membranes with the MF and UF1 selective layers compared to the membrane with the uncoated support. The presence of an obvious significant fouling problem tabulated in Table 7.5 were further analyzed towards the identification of the fouling types by using the experimentally determined clean water fluxes of the fresh, fouled, and cleaned membranes (J_{cwc}, J_{cwf} and J_{cwi} respectively).

Table 7.5 The flux decline of the support, MF and UF1 membranes

Membrane Type	**Flux (L/m^{2}h)**				
	Clean water			**Wastewater**	**Flux Recovery(%)**
	Initial(J_{cwi})	**Final (J_{cwf})**	**Cleaned(J_{cwc})**		
Support	2887	67	1351	41	46
MF	820	233	600	16	73
UF1	270	176	189	11	70

A flux decline analysis is also shown in Table 7.6, where the fractions of total flux decline caused by concentration polarization and fouling are presented. The flux declines due to concentration polarization are 38% for support and about 93% for MF and UF1. The concentration polarization is dominant for total flux decline of MF and UF1.On the other hand the contribution of fouling is as significant as concentration polarization. The flux performance of cleaning the membranes (J_{cwc}) is not high as virgin membranes. (support:2887 to 1351, MF: 820 to 600, UF1: 270 to 189). The differences of J_{cwi} and J_{cwc} shows the irreversible fouling. Table 7.6 shows irreversible fouling type is dominant for support whereas reversible fouling type is dominant for MF and UF1.This estimation is supported by flux recovery (%) of membranes. The flux recovery (%) of support is 46%, MF and UF1 is about70%.

Table 7.6. The concentration polarization and fouling types of Support,MF and UF1 membranes

Membrane Type	Flux Decline (%)				
	Total	Concentration Polarization	Fouling		
			Reversible	Irreversible	Total
Support	98.5	38.8	7	30	34
MF	98	93.1	61	26	71
UF1	95.9	93.75	95	53	98

CHAPTER 8

CONCLUSIONS

In this study the tubular alumina supports were coated slip casting with α alumina, boehmite and titania sols. Selective microfiltration and ultrafiltration (UF1) layers were prepared by α-alumina and boehmite colloidal suspension. The thin top layer and ultrafiltration (UF2) layers were prepared by the packing of nano titania particles from sol-gel method based polymeric sols and hydrosols.

The particle sizes of the sols were determined by DLS-Zetasizer. The sols were dried and micro and nanostructures of the unsupported membranes were investigated with SEM and XRD. The shrinkage behaviour of these room temperature dried unsupported membranes used for the formation of the selective layers were investigated by dilatometry. The heat treatment temperature and the heating rates of the selective layers were selected based on these dilatometric shrinkage/densification curves. The coated and heat treated membrane surfaces were investigated by optical microscope.The ceramic membrane clean water permeability and the separation performance was determined by cross-flow filtration. The wastewaters and permeates were characterized by spectrometer for the determination of various color parameters, suspended solids, turbidity, COD, and TOC.

Selective MF layers were prepared by using 0.5 μm α-alumina suspension with a smaller average particle size than the powder used in the support preparation. Drying temperature and heat treatment rate is important to prepare crack-free MF layers. PVA was used as a drying controll chemical additive and the microfiltration layer was dried at room temperature. MF layer was heat treated at 1200 ^{o}C. The dilatometric curve of dried unsupported 0.5 micron alumina indicated a large percentage of shrinkage between 1000 -1200 ^{o}C. In order to decrease the effect of shrinkage between 1000 ^{o}C to 1200 ^{o}C, heating rate was decreased from 4 ^{o}C to 2 ^{o}C/min. The 0.5 μm alumina (MF) coated selective layer surface heat treated with 2 ^{o}C/min rate were determined to be continuous and crack-free.

UF1 layer was prepared by using a boehmite sol. The avarage particle size of boehmite sol was 42 nm. The addition of acid controlled the stability and gelation of the

boehmite sol. The boehmite sol forms a gel below pH=2. The MF layer was coated by slip casting with boehmite sol. The boehmite coated membrane was dried at room temperature and PVA was used as a DCCA as was used in MF layer consolidation. The UF1 layer heat treatment temperature was 600 ^{o}C. Heat treatment rate was decreased from 4 ^{o}C to 1 ^{o}C/min in order to decrease the shrinkage rate in the 200-400 ^{o}C range.

UF2 layers were prepared by using TiO_2 hydrosols. The avarage particle size of TiO_2 hydrosol was 7nm. The particle size of titania sol was varied by the changing molar ratios of titanium IV isopropoxide: diethanolamine: nitricacid: water: propanol. The TiO_2 hydrosol coated membrane was dried at room temperature and DEA was used as DCCA.

The UF2 layer heat treatment temperature was 400 ^{o}C. Unsupported titania experienced significant shrinkages at about 100^{o}C, 200-300^{o}C and 375-550^{o}C. The main densification range was located in between 375-550^{o}C. The heating rate was choosen as 1^{o}C/min for crack free UF2 selective layer formation.

The clean water fluxes of the support, MF, UF1 and UF2 coated membranes were determined as 2210 L/m^{2}h, 1200 L/m^{2}h, 600 L/m^{2}h, 200 L/m^{2}h at 4 bar.

Wastewater-1 suspended solids contents were reduced by about 60% after the buchner funnel filtration pretreatment. Wastewater-2 and 3 SS contents were reduced about 92-93% by the support filtration pretreatment. The funnel and support treatment decreased MF, UF1 and UF2 fouling. Cumulative percent of color rejection, suspended solid, conductivity, COD and TOC of wastewater-1 permeate were obtained as 90-93%, 99%, 29%, 60%, 79% respectively. Cumulative percent of color rejection, suspended solid, conductivity, COD and TOC wastewater-2 permeate were obtained as 78-87%, 97%, 16.3%, 53%, 66.5% respectively. Cumulative percent of color rejection, suspended solid, conductivity, COD and TOC of wastewater-3 permeate were obtained as 84-88%, 92.6%, 28.5%, 58%, and 75.7% respectively.

A flux decline analysis was also conducted. The flux declines due to concentration polarization are 38% for support and about 93% for MF and UF1. Irreversible fouling type was determined to be dominant for the support whereas reversible fouling was dominant for MF and UF1 coated membranes. The flux recovery (%) of the support was 46% whereas it was about70% for MF and UF1 coated membranes.

Flux decline of the support, MF and UF2 membranes were determined as, 38 L/m^2h, 17 L/m^2h, 12,6 L/m^2h respectively. For wastewater 2, 37 L/m^2h, 48 L/m^2h, 50 L/m^2h. For wastewater3, 25 L/m^2h, 40 L/m^2h, 41 L/m^2h.

REFERENCES

Ahmad A.L., Ismail, S., Bhatia, S., 2005. "Membrane treatment for palm oil mill effluent:Effect of transmembrane pressure and crossflow velocity" Desalination. 179: 245-255.

Angelis, D.L., Cortalezzi, M.M., 2013. "Ceramic membrane filtration of organic compounds:Effect of concentration ,pH, and mixtures interactions on fouling" Seperation and Purification Technology. 118: 762-775.

Benko, K., Drewes, J., Xu, P., Cath,T., 2012. "Use of Ceramic membranes for Produced Water Treatment" National Water Research Institute, USA.

Burgal, J.S., Peeva, L., Marchetti, P., Livingston, A., 2015. "Controlling molecular weight cut-off of PEEK nanofiltration membranes using a drying method" Journal of Membrane Science. 493: 524-538.

Capar, G., Yilmaz, L., Yetis, U., 2006. "Reclamation of acid dye bath wastewater: Effect of pH on nanofiltration performance" Journal of Membrane Science. 281: 560-569.

Capar, G., Yilmaz, L., Yetis, U., 2008. "A membrane-based co-treatment strategy for the recovery of print- and beck-dyeing textile effluents" Journal of Hazardous Materials. 152: 316-323.

Damas, B., Miranda, A., Pia, B., Clar, M.I., Roca, J.A., 2010."Ceramic membrane behavior in textile wastewater ultrafiltration" Desalination. 250: 623-628.

Damas, B., Miranda, A., Pia, B., Clar, M.I., Roca, J.A., 2012. "Application of tubular ceramic ultrafiltration membranes for the treatment of integrated textile wastewaters" Chemical Engineering Journal. 192: 211-218.

DSI,"DSI 2012 faaliyet raporu",2012, www.dsi.gov.tr/docs/stratejik-plan/dsi-2012, (July 2013).

Egerton, T. A., Purnama, H., 2014."Does hydrogen peroxide really accelerate TiO2 UV-C photocatalyzed decolouration of azo-dyes such as Reactive Orange 16" Dyes and Pigments. 101: 280-285.

Ellouze, E.,Tahri, N.,Amar, Ben, R., 2012. "Enhancement of textile wastewater treatment process using Nanofiltration" Desalination. 286: 16–23.

Erdem, I., Ciftcioglu, M., Harsa, S., 2006. "Seperation of whey components by using ceramic composite membranes" Desalination. 189: 87-91.

European Commission, 2010. "Membrane Technologies for water applications" B-109 Brussels, Directorate I- Environtment .

Fan, L., Harris, J.L., 2001. “Influence of the characteristics of natural organic matter on the fouling of microfiltration membranes” Water Research. 35: 4455-4463.

Fersi, C., Gzara, L., Dhambi, M., 2009. “Flux decline study for textile wastewater treatment by membrane processes” Desalination. 244: 321-332.

Gestel, T.V., Kruidhof, H., Blank, D.H.A., Bouwmeester, H. J.M., 2006. “ZrO_2 and TiO_2 membranes for nanofiltration and pervaporation:Part 1. Preparation and characterization of a corrosian reistant ZrO_2 nanofiltration membrane with a MWCO< 300” Journal of Membrane Science . 284: 128-136.

Guillen, G.R., Hoeke, M.V., 2010. “Development and Testing Of Smart Nanofiltration Membranes” USA.

Ivanets, A.I., Ratko, A.I., Azarova, T.A., 2014. “Preparation and properties of microfiltration membranes based on natural crystalline SiO_2” Ceramic International. 40: 12343-12351.

Leslie, G., Antony, A., Le Clech, P., 2012. “Ageing of Polymeric Membranes in Water and Wastewater Treatment” Procedia Engineering. 44: 532-534.

Li, M., Wu, G., Guan, Y., 2011. “Treatment of river water by a hybrid coagulation and ceramic membrane process” Desalination. 280: 114-119.

Lin, Y.S., 2001. “Microporous and dense inorganic membranes: current status and prospective” Seperation Purification Technology. 25: 39-55.

Macedo, A., Duarte, E., Pinho, M., 2011. “The role of concentration polarization in ultrafiltration of ovine cheese whey” Hournal of Membrane Science . 381: 34-40.

Nunes, S.P., Peinemann, V., 2010. “Advanced Polymeric and Organic –Inorganic Membranes for Pressure-Driven Processes” Comprehensive Membrane Science and Engineering . 1: 113-129.

Potdar, A., Shukla, A., Kumar, A., 2002. “Effect of gas phase modification of analcime zeolite composite membrane on separarion of surfactant by ultrafiltration” Journal of Membrane Science. 210: 209-225.

Schrank, G.S., Dos Santos, J.N.R., Souza, D.S., Souza, S.E., 2007. “Decolourisation effects of Vat Green 01 textile dye and textile wastewater using H_2O_2/UV process” Journal of Photochemistry and Photobiology. 186: 125-129.

Tsuru, T., Sudoh, T., Yoshioka, T., Asaeda, M., 2000. “Nanofiltration in non-aqueous solutions by porous silica-zirconia membranes” Journal of Membrane Science. 185: 253-261.

Tsuru, T., 2008. “Nano/Subnano-tuning of porous ceramic membranes for molecular seperation” Journal of Sol-Gel Science Technology. 46: 349-361.

TUIK,“Imalat Sanayi Su Göstergeleri”,2012, www.tuik.gov.tr/PreTablo.do?alt_id=1019 (July 2013).

Uzal, N., Yilmaz, L., Yetis, U., 2009. “Microfiltration/ultrafiltration as pretreatment for reclamation of rinsing waters of indigo dyeing” Desalination. 240: 198-208.

Van Der Burggen, B., Curcio, E., Drioli, E., 2004. “Process intensification in the textile industry : the role of membrane technology” Journal of Environmental Management. 73: 267-274.

Vrijenhoek, E.M., Elimelech, M., 2001. “Influence of membrane surface properties on initial rate of colloidal fouling of reverse osmosis and nanofiltration membranes” Journal of Membrane Science . 188: 115-128.

Yang, C., Zhang, G., Xu, N., Shi, J., 1998. “preparation and application in oil-water seperation of ZrO_2/α-Al_2O_3 MF membrane” Journal of Membrane Science. 142: 235-243.

Yoldas, B., 1975. “Alumina sol preparation from Alkoxide” American Ceramic Society Bulletin. 513: 289-290.

Zhong,Z., Li, D., Zhang, B., Xing, W., 2012. “Membrane surface roughness characterization and its influence on ultrafine partice adhesion” Seperation and Purification Technology . 90: 140-146.

Ziedler, S., Puhlfürss, P., Katzel, U., Voigt, I., 2014. “Preparation and characterization of new low MWCO ceramic nanofiltration membranes for organic solvents” Journal of Membrane Science. 470: 421-430.